



**HAL**  
open science

## A comparative study of total alkalinity and total inorganic carbon near tropical Atlantic coastal regions

Frédéric Bonou, Carmen Medeiros, Carlos Noriega, Moacyr Araujo, Aubains Hounsou-Gbo, Nathalie Lefèvre

### ► To cite this version:

Frédéric Bonou, Carmen Medeiros, Carlos Noriega, Moacyr Araujo, Aubains Hounsou-Gbo, et al.. A comparative study of total alkalinity and total inorganic carbon near tropical Atlantic coastal regions. *Journal of Coastal Conservation: planning and management*, 2022, 26 (4), pp.31. 10.1007/s11852-022-00872-5 . hal-04609952

**HAL Id: hal-04609952**

**<https://hal.science/hal-04609952v1>**

Submitted on 18 Jun 2024

**HAL** is a multi-disciplinary open access archive for the deposit and dissemination of scientific research documents, whether they are published or not. The documents may come from teaching and research institutions in France or abroad, or from public or private research centers.

L'archive ouverte pluridisciplinaire **HAL**, est destinée au dépôt et à la diffusion de documents scientifiques de niveau recherche, publiés ou non, émanant des établissements d'enseignement et de recherche français ou étrangers, des laboratoires publics ou privés.

## A comparative study of total alkalinity and total inorganic carbon near tropical Atlantic coastal regions

Bonou Frédéric <sup>1,2,8,\*</sup>, Medeiros Carmen <sup>7</sup>, Noriega Carlos <sup>3</sup>, Araujo Moacyr <sup>3,4</sup>,  
Hounsou-Gbo Aubains <sup>5</sup>, Lefèvre Nathalie <sup>6</sup>

<sup>1</sup> Laboratoire de Physiques et Applications, LPA/ Université Nationale Des Sciences Technologies, Ingénierie Et Mathématiques (UNSTIM), Cotonou, Benin

<sup>2</sup> International Chair in Mathematical Physics and Applications (ICMPA-Unesco Chair), Université d'Abomey-Calavi (UAC), Cotonou, Bénin

<sup>3</sup> Center for Studies and Tests On Risk and Environmental Modeling (CEERMA), Federal University of Pernambuco (UFPE), Av. Arquiterura s/n, Recife, 50740-550, Brazil

<sup>4</sup> Brazilian Research Network On Global Climate Change, Rede CLIMA, S. José Dos Campos, SP, Brazil

<sup>5</sup> Instituto de Ciências do Mar (LABOMAR), Universidade Federal do Ceará (UFC), Av. da Abolição, 3207, CE: 60165-081, Fortaleza, Brazil

<sup>6</sup> Université Pierre Et Marie Curie, 4 place Jussieu, 75252 Cedex 05, Paris, France

<sup>7</sup> Laboratório de Oceanografia Física Estuarina e Costeira (LOFEC/DOCEAN/CTG), Federal University of Pernambuco, Av. Arquiterura s/n, 50740-550, Recife, Brazil

<sup>8</sup> Institut de Recherches Halieutiques et Océanologiques du Bénin, IRHOB, Cotonou, Benin

\* Corresponding author : Frédéric Bonou, email address : [fredericbonou@yahoo.fr](mailto:fredericbonou@yahoo.fr)

### Abstract :

This paper is based on a comparison of the carbon parameters at the western and eastern borders of the tropical Atlantic using data collected from 55 cruises. Oceanic and coastal data, mainly total alkalinity (TA), total dissolved inorganic carbon (CT), sea surface salinity (SSS) and sea surface temperature (SST), were compiled from different sources. These data were subdivided into three subsets: oceanic data, coastal data and adjacent to the Brazilian (western) and African coastal areas (eastern) data. Significant differences between the TA data ( $2099.4 \pm 286.4 \mu\text{mol kg}^{-1}$ ) at the western and eastern edges ( $2198 \pm 141.9 \mu\text{mol kg}^{-1}$ ) were observed. Differences in the CT values between the western edge ( $1779.6 \pm 236.4 \mu\text{mol kg}^{-1}$ ) and eastern edge ( $1892.2 \pm 94.2 \mu\text{mol kg}^{-1}$ ) were also noted. This pattern was due to the different variabilities in the carbon parameters between the eastern and western border coastal areas and to the biogeochemistry that drives these parameters. In the western coastal area, the physical features of the continental carbon and oceanic waters mixing with the freshwater that flows from the Amazon and Orinoco Rivers to the South American coast are different than the physical features of the water that flows from the Congo, Volta and Niger Rivers in the eastern region. Applying the TA empirical relationship to TA with values of  $\text{SSS} < 35$  in the western and eastern regions leads to a higher root mean square error (rmse) in the eastern and western regions. Therefore, most of the existing TA empirical relationships are most useful at the regional scale due to the difference in the water properties of each region. The relationships of TA and CT determined in the western and eastern regions do not reproduce in situ data well, especially at the adjacent edges. This difference is explained by the difference between the African and Brazilian coasts in terms of their carbon parameter characteristics and processes

---

responsible for their variation. Based on the mixing model, it has been shown that the primary productivity in the eastern region is higher than that in the western region. This is one of the reasons why the carbon parameters are higher in the eastern region. For each region studied, an equation for TA is introduced in this study.

**Keywords** : Carbonate system, Tropical Atlantic, West Africa, Brazilian border, Rivers, Coastal regions, Chemical oceanography

1  
2  
3  
4  
5  
6 **Highlights**

- 7 - Compiled three decades of carbon data cruises.  
8  
9 - Investigated TA/C<sub>T</sub> differences in tropical Atlantic coastal zones.  
10  
11 - Significant difference between TA/C<sub>T</sub> data from the African and Brazilian coastal areas were  
12 determined.  
13  
14 - High influence of C<sub>T</sub> in the eastern region compared to that in the western region of the tropical  
15 Atlantic Ocean was recorded.  
16  
17 - Four empirical equations were proposed for the four regions studied.  
18  
19  
20  
21  
22  
23

24 **1. Introduction**

25  
26  
27 Between the African and South American continents, the tropical Atlantic receives approximately  
28  
29 0.1 Pg C yr<sup>-1</sup> of carbon, 0.046 Pg C yr<sup>-1</sup> of dissolved organic carbon (DOC), and 0.053 Pg C yr<sup>-1</sup>  
30  
31 of dissolved inorganic carbon total (C<sub>T</sub>) (Huang et al., 2012). According to Araujo et al. (2014),  
32  
33 13.2% of the C<sub>T</sub> and 27.3% of the DOC global values are transported from rivers into the world's  
34  
35 oceans. Furthermore, rivers provide 0.8-1.33 Pg C to oceans worldwide, of which ~ 0.53 Pg C is  
36  
37 transported from tropical rivers (30°N- 30°S) to adjacent estuarine-coastal systems (Huang et al.,  
38  
39 2012).  
40  
41  
42

43 In the tropical Atlantic, the Amazon River is the largest river, flowing from west to east, while the  
44  
45 Congo River is the second largest river, which has a local dynamic in this area (Cai et al., 2008).  
46  
47

48 The transport of terrestrial, oceanic and atmospheric carbon in the global carbon cycle is influenced  
49  
50 by rivers. Freshwater is generally rich in terrestrial and atmospheric carbon and is transported to  
51  
52 the ocean through rivers (Araujo et al., 2014). The high nutrient concentrations transported by the  
53  
54 river flux within the continental shelf and adjacent oceanic region increase primary production and  
55  
56 can lead to the absorption of CO<sub>2</sub> (Körtzinger, 2003; Regnier et al., 2013). Previous studies have  
57  
58  
59  
60  
61  
62  
63  
64  
65

1  
2  
3  
4 also revealed that South American estuaries (western region) and African estuaries (eastern region)  
5  
6 are carbon sources ( $+10.6 \pm 7$  mmol  $\text{m}^{-2} \text{day}^{-1}$  and  $+7.0$  mmol  $\text{m}^{-2} \text{day}^{-1}$ , respectively) for the  
7  
8 tropical Atlantic (Araujo et al., 2014). Therefore, the coastal regions adjacent to rivers are regions  
9  
10 with highly variable  $\text{CO}_2$  parameters due to the carbon input that occurs through the discharge of  
11  
12 rivers into oceanic regions. The amount of carbon from the continental input at the separate edges  
13  
14 (eastern and western) can influence the carbonate system, such as the total alkalinity (TA) and total  
15  
16 dissolved inorganic carbon ( $\text{C}_T$ ). It is necessary to collect data at these edges to better understand  
17  
18 the variability of these parameters.  
19  
20  
21  
22

23  
24 Important processes can be responsible for carbonate chemistry changes in the ocean, and they can  
25  
26 be described by considering the changes in  $\text{C}_T$  and TA. The invasion of  $\text{CO}_2$  from (or the release  
27  
28 of  $\text{CO}_2$  to) the atmosphere increases (or decreases)  $\text{C}_T$  while TA remains constant, leading to a rise  
29  
30 and drop of  $[\text{CO}_2]$ , respectively, with opposite changes in pH (since  $\text{CO}_2$  is a weak acid).  
31  
32 Respiration and photosynthesis led to the same trends, except that TA changed slightly due to  
33  
34 nutrient release and uptake.  $\text{CaCO}_3$  precipitation decreases  $\text{C}_T$  and TA at a ratio of 1:2 and,  
35  
36 counterintuitively, increases  $[\text{CO}_2]$ , although inorganic carbon is reduced.  
37  
38  
39

40  
41 The spatial distribution of  $\text{CO}_2$  and  $\text{C}_T$  in the surface ocean is mainly explained by the temperature-  
42  
43 dependent solubility of  $\text{CO}_2$  on interannual timescales. Because of increased solubility at low  
44  
45 temperatures, warm low-latitude surface water retains less  $\text{CO}_2$  ( $\sim 10$   $\mu\text{mol kg}^{-1}$ ) and  $\text{C}_T$  ( $\sim 2000$   
46  
47  $\mu\text{mol kg}^{-1}$ ) than cold high-latitude surface water ( $\text{CO}_2 \sim 15$   $\mu\text{mol kg}^{-1}$  and  $\text{C}_T \sim 2100$   $\mu\text{mol kg}^{-1}$ ).  
48  
49 Significant deviations from these broad trends may occur locally and on seasonal time scales due  
50  
51 to changes in salinity and processes such as biological activity, upwelling, temperature variations,  
52  
53 river runoff, and other activities that alter  $\text{C}_T$  and TA.  
54  
55  
56

57  
58 Some equations have been developed in recent decades to determine the carbon parameters TA,  $\text{C}_T$   
59  
60 and fugacity ( $f\text{CO}_2$ ) as functions of physical and other parameters that are easily measurable and  
61  
62  
63  
64  
65

1  
2  
3  
4 accessible (Takahashi et al., 2014, Lefèvre et al., 2010, Koffi et al., 2010). Linear regression  
5  
6 relationships can be a good option to estimate carbon parameters. Empirical equations also present  
7  
8 large uncertainties in data due to the complexity of the carbon parameters in coastal areas. Although  
9  
10 empirical equations are useful to reproduce carbon parameters, they have spatial and temporal  
11  
12 limitations for reproducing carbon parameters well in a whole oceanic basin. There have been few  
13  
14 studies that focus on the tropical Atlantic with an emphasis on the contribution of river discharge  
15  
16 to carbon. In 2006, other authors used the relationship TA vs. SSS (sea surface salinity) and SST  
17  
18 (sea surface temperature) in the tropical Atlantic (30°S-30°N) for oceanic regions with the SSS  
19  
20 criterion (greater than 31) (Lee et al., 2006). This empirical relationship cannot be used for data  
21  
22 with low SSS in these regions with higher discharge due to major rivers. In the tropical Atlantic,  
23  
24 Takahashi et al. (2014a) determined and used only one empirical relationship of TA regression for  
25  
26 the whole tropical Atlantic basin; this relationship is similar to the one determined by Lefèvre et  
27  
28 al. (2010), specifically for the Amazon region. In the same year, Koffi et al. (2010) determined a  
29  
30 different TA relationship in the eastern Gulf of Guinea, with a slope that was highly different from  
31  
32 that determined in Lefèvre et al. (2010) and Takahashi et al. (2014a). Due to the spatiotemporal  
33  
34 variability, in the western region, an empirical relationship of  $C_T$  was obtained by Bonou et al.  
35  
36 (2016a) using SSS and time variation (year), while in the eastern region, Koffi et al. (2010)  
37  
38 determined an empirical relationship of  $C_T$  using SST and SSS (**Table 1**). It is desirable to continue  
39  
40 studying the performance of linear regression, multiple regression or other methods to obtain a  
41  
42 better estimation of the carbon parameters. The compilation of many data cruises, within the  
43  
44 context of acquiring new observation data, is a good means to determine existing relationships in  
45  
46 order to have robust equations that are adaptable to the regions, leading to smaller uncertainties.  
47  
48  
49  
50  
51  
52  
53  
54  
55  
56  
57  
58  
59

60 **Table 1**

1  
2  
3  
4  
5  
6  
7 Data from different sources are compiled from different oceanographic data cruises (1983-2014)  
8  
9 to compare the TA and  $C_T$  variations in the western and eastern tropical Atlantic, mainly in coastal  
10  
11 areas adjacent to rivers. The compilation of several data cruises was used to test the reliability of  
12  
13 the existing relationships and to reproduce the TA/ $C_T$  distribution in these transition regions. A  
14  
15 comparative study was performed to emphasize the limits and differences in the variation in TA/ $C_T$   
16  
17 at the tropical Atlantic borders.  
18  
19  
20  
21  
22

## 23 **2. Material and Methods**

### 24 **2.1. Database and methodology**

25  
26 All available cruise data were extracted from oceanographic and voluntary merchant ships (20°S-  
27  
28 20°N, 70°W-15°E) in the tropical Atlantic, which is the study area where in situ data TA,  $C_T$ , SST  
29  
30 and SSS were sampled and measured (**Figure 1**). In Figure 1, the data are shown in red and green  
31  
32 for SSS<35 (points in black indicate SSS>35). The dataset was acquired from 1983 to 2014 through  
33  
34 55 campaigns (**Table 2**) completed with those used in Bonou et al. (2016). Conductivity,  
35  
36 temperature and depth data acquired with CTD and bottle samples during those surveys were  
37  
38 obtained from the Carbon Dioxide Information and Analysis Center  
39  
40 ([http://cdiac.ornl.gov/oceans/bottle\\_discrete.html](http://cdiac.ornl.gov/oceans/bottle_discrete.html)).  
41  
42  
43  
44  
45  
46  
47  
48  
49

### 50 **Figure 1 (Single Column)**

### 51 **Table 2**

1  
2  
3  
4 The TA and C<sub>T</sub> data used in this study were obtained from data cruises and were determined by  
5  
6 potentiometric titration from either a full curve (“Full”) or a single-point (“1-point”) titration.  
7

8  
9 The SSS database was obtained from an updated version of SSS data from 2013 by Reverdin et al.  
10  
11 (2007). These data were used as indicators for determination of the area affected by freshwater due  
12  
13 to rivers in the tropical Atlantic. The monthly SST data were extracted from the Objectively  
14  
15 Analyzed air-sea Fluxes Project (OAFlux) database (with 1° of longitude and 1° of latitude). The  
16  
17 SST data used in this study were acquired from 1958-2014, and the data are available on the Woods  
18  
19 Hole Oceanographic Institution (WHOI) website at [oaflux.whoi.edu](http://oaflux.whoi.edu). The OAFlux project provides  
20  
21 a synthesized product generated from the reanalysis datasets NCEP1, NCEP2, ERA40 and ERA  
22  
23 (Yu and Weller, 2007, Yu et al., 2008).  
24  
25  
26  
27

28 The TA and C<sub>T</sub> relationships used were determined by different authors (see **Table 1**) to verify  
29  
30 their limits to reproduce data compared to the observation data, especially at the eastern and  
31  
32 western borders.  
33  
34  
35  
36  
37

## 38 **2.2. Statistical analysis**

39  
40 Statistical analysis and the Mann–Whitney test were used to compare two sets of data (TA, C<sub>T</sub>,  
41  
42 SST, and SSS) from different areas (western tropical Atlantic and eastern tropical Atlantic) to  
43  
44 determine the difference between the carbon parameters (TA and C<sub>T</sub>) in the different localities.  
45  
46 Linear regression methods were applied to determine and test the connections between the physical  
47  
48 parameters and carbon parameters; this method was also used to observe the best fit that matched  
49  
50 the observation data. To compare these different relationships, the root mean square error (rmse)  
51  
52 was calculated as follows:  
53  
54  
55  
56  
57

$$58 \text{ rmse} = \left[ \frac{1}{n-1} \times \sum_{i=1}^n (X_i - Y_i)^2 \right]^{1/2} \quad (3);$$

59  
60  
61  
62  
63  
64  
65



1  
2  
3  
4 where  $X_i$  is the observed value and  $Y_i$  is the modeled value at time/place  $i$ .

5  
6 The Kruskal–Wallis test was used to identify significant differences ( $\alpha=0.05$ ) between all regions.

7  
8 Additionally, Dunn’s test was applied to identify significant differences between borders (NW,  
9  
10 NE, SW, and SE, for  $\alpha=0.05$ ) and between hemispheres.  
11  
12  
13  
14

### 15 16 **3. Results**

#### 17 18 **3.1. The distribution of SSS and SST anomalies in the tropical Atlantic**

19  
20 Standard deviations of SSS anomalies computed for the period from 1970-2013 using the database  
21  
22 from Reverdin et al. (2007) actualized in 2013 allowed us to map the areas under distinct degrees  
23  
24 of influence of freshwater input due to river discharge and/or precipitation (Figure 2). The regions  
25  
26 of influence of freshwater input due to river discharge and/or precipitation (Figure 2). The regions  
27  
28 presenting high SSS variability ( $SD>1$ ) along South America corresponded to coastal areas  
29  
30 adjacent to the mouths of the Amazon and Orinoco Rivers and areas along the African coastal  
31  
32 border adjacent to the Congo, Niger and Volta River mouths. Lower variations in SSS anomalies  
33  
34 were observed in the oceanic zone and along coastal areas not receiving large river discharge, as is  
35  
36 the case for the NE-Brazilian coast and the northern coast of Africa. The São Francisco River in  
37  
38 NE Brazil (**Figure 2**) does not induce significant variation in the SSS due to the presence of  
39  
40 numerous dams of hydroelectric plants along its course, drastically reducing its flow despite the  
41  
42 extension of its drainage basin.  
43  
44  
45  
46  
47  
48  
49

#### 50 51 **Figure 2 (Single Column)**

52  
53  
54  
55 The SST distribution in the study area presents a seasonal zonal pattern with less variable values  
56  
57 along the western Atlantic relative to that of the eastern Atlantic. SST along the South American  
58  
59 coast varies from 26 to 28 °C in January and between 25 and 29 °C in July. Along the African  
60  
61  
62  
63  
64  
65

1  
2  
3  
4 coast, SST is higher ( $>27\text{ }^{\circ}\text{C}$ ) in the eastern Atlantic ( $0^{\circ}$  to  $5^{\circ}\text{N}$ ) in January and lower ( $<26\text{ }^{\circ}\text{C}$ ) in  
5  
6 coastal areas between the equator and  $10^{\circ}\text{S}$  in July (**Figure 3**).

### 11 **Figure 3 (Single Column)**

12  
13  
14 The annual amplitude of the SST in the western Atlantic (including  $20^{\circ}\text{S}$ - $20^{\circ}\text{N}$ ;  $70^{\circ}\text{W}$ - $30^{\circ}\text{W}$ ) was  
15  
16  $3.0\text{ }^{\circ}\text{C}$ . However, in the eastern Atlantic (including  $20^{\circ}\text{S}$ - $20^{\circ}\text{N}$ ;  $20^{\circ}\text{W}$ - $15^{\circ}\text{E}$ ), the amplitude of the  
17  
18 SST was  $5.7\text{ }^{\circ}\text{C}$  (**Figure 3,4**).

### 23 **Figure 4 (1.5 Column)**

24  
25  
26  
27  
28 A subset division of the tropical Atlantic Ocean into four regions (NW, SW, NE and SE) is included  
29  
30 according to the variability in the SST climatological. This division sought to differentiate the  
31  
32 variations between the hemispheres and the continental borders (**Figure 4**).

33  
34  
35 The Kruskal–Wallis test showed significant differences ( $\alpha=0.05$ ;  $p=0.0007$ ) between all regions.  
36  
37 Additionally, Dunn’s test showed significant differences between borders (NW  $\neq$  NE;  $\alpha=0.05$ ;  
38  
39  $p=0.012$  and SW  $\neq$  SE;  $\alpha=0.05$ ;  $p=0.008$ ) and between hemispheres (NW  $\neq$  SW;  $\alpha=0.05$ ;  $p=0.009$   
40  
41 and NE  $\neq$  SE;  $\alpha=0.05$ ;  $p=0.003$ ).

42  
43  
44 For  $\text{SSS}<35$  (freshwater influence), the statistical test also confirmed a significant difference  
45  
46 between the SST values of the eastern and western regions (Mann–Whitney test,  $p=0.0001$ ;  $\alpha =$   
47  
48  $0.05$ ).

### 55 **3.2. TA and $C_T$ in the tropical Atlantic**

56  
57  
58 Three hundred ninety-two in situ coastal data samples of TA,  $C_T$ , SSS and SST from the western  
59  
60 region, represented in red, were used in this study and compared to 103 data samples of TA,  $C_T$ ,

1  
2  
3  
4 SSS and SST from the eastern region, represented in green (**Figure 1**). All these data were obtained  
5  
6 under the criterion of SSS being less than 35 psu. A significant difference was observed when the  
7  
8 selected TA and  $C_T$  data (in red points) from the western Atlantic were compared with TA and  $C_T$   
9  
10 data (green points) from the eastern tropical Atlantic. At the western edge, the average value of TA  
11  
12 ( $2099.4 \pm 286.4 \mu\text{mol kg}^{-1}$ ) was obtained; this value was lower than the value obtained from the  
13  
14 eastern tropical Atlantic ( $2198 \pm 141.9 \mu\text{mol kg}^{-1}$ ) (**Table 3**), while the standard deviation indicated  
15  
16 a higher variation in TA in the western region than that obtained in the eastern region (Mann–  
17  
18 Whitney test,  $p = 0.0008$ ,  $\alpha = 0.05$ ). For the  $C_T$  variable, ( $1892.2 \pm 94.2 \mu\text{mol kg}^{-1}$ ) and ( $1779.6 \pm$   
19  
20  $236.4$ )  $\mu\text{mol kg}^{-1}$  are the mean values and the standard deviation obtained, respectively, at the  
21  
22 eastern and western borders. The standard deviation on CT in the western border was higher than  
23  
24 that of the eastern border, showing higher variation in TA and CT in South America than in the  
25  
26 African border (Mann–Whitney test,  $p = 0.00002$ ,  $\alpha = 0.05$ ).  
27  
28  
29  
30  
31  
32  
33  
34  
35

### 36 **Table 3**

37  
38  
39 This result supports the higher average values of TA and  $C_T$  (**Table 3**) in the eastern region Koffi  
40  
41 et al. (2010) and the higher TA and CT values in the Gulf of Guinea, especially in this upwelling  
42  
43 region (**Figure 4**).  
44  
45  
46  
47  
48

### 49 **3.3. Relevance and limitation of existing relations for TA and $C_T$ in the tropical Atlantic.**

50  
51 The relationships proposed by Lefèvre et al. (2010), Koffi et al. (2010) and Bonou et al. (2016a)  
52  
53 (**Table 4**) were used to compute TA and  $C_T$  and to observe their spatial relevance and limitations  
54  
55 in the tropical Atlantic. The data in red and green samples have SSS values lower than 35, while  
56  
57 the data in black correspond to those of the regions where SSS is higher than 35 (**Figure 1**).  
58  
59  
60  
61  
62  
63  
64  
65

1  
2  
3  
4 **Table 4**  
5

6 Observations of  $SSS < 35$  in the western border are due to the higher influence of rivers and  
7 freshwater due to the retroflexion of Amazonian waters by the North Brazilian Current (NBC) and  
8 into the NECC, which is beyond the influence of rainfall in the equatorial region due to the ITCZ  
9 (intertropical convergence zone). In this region, the empirical relationship proposed by Lefèvre et  
10 al. (2010) represents the TA observations better than the relationships proposed by Koffi et al.  
11 (2010) (**Figure 5A**). The standard deviation of TA from Lefèvre et al. (2010) was  $28.6 \mu\text{mol.kg}^{-1}$ ,  
12 while that obtained for TA by Koffi et al. (2010) was  $64.8 \mu\text{mol.kg}^{-1}$  (**Table 4**). The greatest  
13 discrepancies occur for data with  $SSS < 30$ .  
14  
15  
16  
17  
18  
19  
20  
21  
22  
23  
24  
25  
26  
27

28 **Figure 5 (Single Column)**  
29  
30  
31  
32

33 The opposite trend was observed in the eastern region, where the relationship described in Koffi  
34 et al. (2010) is better at reproducing the observation data than that described in Lefèvre et al.  
35 (2010) (**Figure 6**). The rmse value of TA was  $12.5 \mu\text{mol kg}^{-1}$ , which was obtained from the  
36 relationship from Koffi et al. (2010) in the eastern region. This rmse value TA is almost two  
37 times lower than that obtained with the relationship of Lefèvre et al. (2010) (**Table 4**). This result  
38 agrees with that obtained in Lefèvre et al. (2010), which showed the best fit of TA with SSS  
39 when using Koffi et al. (2010).  
40  
41  
42  
43  
44  
45  
46  
47  
48  
49  
50  
51  
52

53 **Figure 6 (1.5 Column)**  
54  
55  
56  
57

58 **3.4. Biological processes**  
59  
60  
61  
62  
63  
64  
65

1  
2  
3  
4 In the western and eastern tropical Atlantic, biological consumption is one of the processes that  
5  
6 influences the variation in the carbon parameters around tropical edges (Cooley et al., 2007; da  
7  
8 Cunha et al., 2013; Araujo et al., 2014).  
9

10  
11 As explained above, the surface  $C_T$  concentration is influenced by lateral and vertical mixing of  
12  
13 water with different levels of  $C_T$  (the transport effect), photosynthesis and oxidation of organic  
14  
15 matter (the biological effect) and changes in temperature and salinity (Takahashi et al., 1993; Lee  
16  
17 et al., 2000). However, these effects are directly or indirectly correlated with SST, but the trends  
18  
19 often differ seasonally and geographically.  
20  
21

22  
23 According to Koffi et al. (2010), equatorial upwelling and coastal upwelling along the eastern  
24  
25 boundary merge to form a cold tongue during the main upwelling season, and the cold tongue  
26  
27 undergoes advection westward by the South Equatorial Current (SEC). This cold tongue transports  
28  
29  $CO_2$ -rich waters, and  $fCO_2$  increases as the surface water temperature increases toward the west.  
30  
31

32  
33 The Guinea Current (GC) and SEC are influenced by several fluvial contributions, including the  
34  
35 Volta River ( $4^\circ N-0^\circ$ ), Niger River ( $3^\circ N, 8^\circ E$ ) and Congo River ( $-6^\circ S, 12^\circ E$ ) (Koffi et al., 2010).  
36  
37

38  
39 The eastern border is strongly affected by biological activity (NE and SE). The average  $C_T$  was  
40  
41  $2056 \mu mol kg^{-1}$ , which is close to that of the Atlantic Ocean, as indicated by Millero (2006).  
42

43  
44 The satellite data through the MODIS-Aqua sensor were used for the study region. The highest  
45  
46 concentrations of chlorophyll-*a* are observed in the coastal regions near the Amazon River, Orinoco  
47  
48 River, Congo River and NW Africa (coastal upwelling) (**Figure 7**).  
49

## 50 51 52 53 **4. Discussion**

### 54 55 **4.1. Analysis of the regions influenced by tropical Atlantic Rivers**

56  
57  
58  
59  
60  
61  
62  
63  
64  
65

1  
2  
3  
4 The standard deviation distribution of anomalies was used by Bonou et al. (2016a) to identify  
5  
6 regions with higher variations in the variables considered. In our work, this method was applied to  
7  
8 investigate the subregions of the tropical Atlantic characterized by higher variations in SSS (**Figure**  
9  
10 **2**). The fact that almost all the regions of the tropical Atlantic presenting large SDs of SSS  
11  
12 anomalies were located near tropical rivers presenting high discharge corroborates that this method  
13  
14 is robust to identifying the influence of its discharge on salinity.  
15  
16

17  
18 The standard deviation of SSS was an anomaly with values between 0.2 and 2.0 for the coastal  
19  
20 regions of the study area. There is a significant difference between the SSS anomalies (Mann–  
21  
22 Whitney test,  $p=0.0005$ ;  $\alpha = 0.05$ ) at the western and eastern borders of the tropical Atlantic. The  
23  
24 hydric balance of the Amazon and Orinoco Rivers at the western edge is greater than the balance  
25  
26 of the Congo, Niger and Volta Rivers at the eastern border (Dai and Trenberth, 2002; Cai et al.,  
27  
28 2008; da Cunha et al., 2013; Araujo et al., 2014). According to Bonou et al. (2016a), in the tropical  
29  
30 Atlantic, the variation in SSS is higher in the western region, with SSS values between 1 and 38.  
31  
32

33  
34 The western tropical Atlantic shows a higher variability in SSS and a less pronounced seasonal  
35  
36 variability in SST. On the other hand, the eastern tropical Atlantic presents a lower variability in  
37  
38 SSS but a strong seasonal variability in SST (**Figures 2, 3 and 4**). This area experiences coastal  
39  
40 upwelling (Schneider et al., 1997; Dale et al., 2002), where a rise in cold-water masses rich in  
41  
42 nutrients and CO<sub>2</sub> is observed and surface coastal water is pushed offshore by Ekman divergence.  
43  
44

45  
46 The SSS is a physical parameter that has a high correlation with carbon parameters, and its  
47  
48 variability is believed to impact carbon parameters. In the Tropical Atlantic, the SSS is highly  
49  
50 correlated with TA and CT (Bonou et al. (2016a), Koffi et al. (2010), Lefèvre et al. (2010);  
51  
52 therefore, the stronger influence of the Amazon and Orinoco Rivers in the western tropical Atlantic  
53  
54 is one explanation for the difference observed in the carbon parameters between the eastern and  
55  
56 western regions.  
57  
58  
59  
60  
61

#### 4.2. Pertinence of existing relations to the tropical Atlantic.

The results presented in **Figures 5A** and **5B** show that the relationships from Lefèvre et al. (2016) are adapted in the western tropical Atlantic region mainly in the Amazon and Orinoco Rivers, while the relationship from Koffi et al. (2010) reproduces the observations in the eastern tropical Atlantic well, mainly in the Gulf of Guinea.

In the central basin of the tropical Atlantic, the results with  $SSS \geq 35$  showed that the behavior was very close between the two empirical relationships (**Figure 5C**). The relationship from Lefèvre et al. (2016) had a slightly higher rmse value than that obtained from the relationship from Koffi et al. (2010) (20.5 and 19.2  $\mu\text{mol kg}^{-1}$ , respectively). According to these results, the use of the two empirical relationships yielded similar TA values in the central region when  $SSS \geq 35$  psu.

Almost all TA data with  $SSS \geq 37$  are clustered around the green line, which is the line represented by the relationships from Koffi et al. (2010). Data with  $SSS \geq 37$  are located in the SEC region (**Figure 6**), which extends to the western part. This result means that the relationship from Koffi et al. (2010), as determined in the eastern region, can be extended into the western part of the SEC.

Analysis of the proposed relationships used to determine  $C_T$  is more complicated, at least regarding its graphical representation. In the eastern region, Koffi et al. (2010) determined  $C_T$  relationships using SSS and SST, while Bonou et al. (2016a) determined a  $C_T$  relationship using only the SSS function but still considered its temporal variation (**Table 3**) in the western tropical Atlantic region.

The  $C_T$  relationships in both regions (western and eastern) do not depend only on SSS and TA relationships. In this case,  $C_T$  cannot be estimated only as a function of a single SSS parameter, and the statistical results are presented in **Table 4** (Bonou et al., 2016b).

1  
2  
3  
4 In the western tropical Atlantic, the rmse value was obtained from the estimated  $C_T$  derived from  
5  
6 Bonou et al. (2016a), and this value was  $41.1 \mu\text{mol kg}^{-1}$  considering that the relationship from Koffi  
7  
8 et al. (2010) gives  $47.9 \mu\text{mol kg}^{-1}$  as the rmse value. In the eastern region, the rmse value obtained  
9  
10 from the estimated  $C_T$  relationship from Koffi et al. (2010) was  $28.11 \mu\text{mol kg}^{-1}$ , while from Bonou  
11  
12 et al. (2016a), the rmse value was  $29.6 \mu\text{mol kg}^{-1}$ . In the oceanic region ( $\text{SSS} \geq 35$ ), the rmse values  
13  
14 were also similar between the two empirical relationships ( $34.7$  and  $35.1 \mu\text{mol kg}^{-1}$  for Koffi et al.  
15  
16 (2010) and Bonou et al. (2016a), respectively). In fact, the greatest variation in SST observed in  
17  
18 the eastern edge of the basin contributes to the  $C_T$  equation since SST is one of the key state  
19  
20 variables that influence the carbon cycle in this region (Lefèvre et al., 2008; Koffi et al., 2010,  
21  
22 Bonou et al., 2016b). On the other hand, the empirical relationships of  $C_T$  proposed for the western  
23  
24 edge do not consider SST because their variation is lower at the western edge than in the eastern  
25  
26 region (Lefèvre et al., 2010; Ibánhez et al., 2015; Bonou et al., 2016a). According to Key et al.  
27  
28 (2004), the surface  $C_T$  distribution is affected by physical processes; however, the pattern is more  
29  
30 similar to that of nutrients (e.g., nitrate) than to that of salinity. This is because  $C_T$  concentrations  
31  
32 are more strongly affected by biology than TA concentrations.  
33  
34  
35  
36  
37  
38  
39  
40  
41  
42

### 43 **4.3. Lithological composition of basins and influence of plumes**

44  
45 The different rock types that dominate the river basins influence the input of  $\text{CO}_2$  through rock  
46  
47 weathering and through riverine transport of inorganic carbon to the ocean. The chemical erosion  
48  
49 of inorganic materials consists of dissolving or hydrolyzing primary minerals of rocks and soils.  
50  
51 The chemical reactions require  $\text{CO}_2$  and release  $C_T$  (mainly as  $\text{HCO}_3^-$ ). Thus, different rock types  
52  
53 have different  $\text{CO}_2$  consumption rates. According to Amiotte-Suchet et al. (2003), high  $\text{CO}_2$   
54  
55 consumption rates are observed in carbonate rocks, moderate  $\text{CO}_2$  consumption rates are observed  
56  
57 in basalts plus shales, and low  $\text{CO}_2$  consumption rates are observed in shales plus and  
58  
59  
60  
61  
62  
63  
64  
65



1  
2  
3  
4 sands/sandstones. Thus, the Amazon and Orinoco Rivers have high CO<sub>2</sub> consumption rates, and  
5  
6 the Congo and Niger Rivers have moderate and low CO<sub>2</sub> consumption rates. Araujo et al. (2014)  
7  
8 observed that the contribution of the mean CO<sub>2</sub> fluxes consumed by the total HCO<sub>3</sub><sup>-</sup> river flux was  
9  
10 82 and 88% for the western border and eastern border, respectively. These authors also indicated  
11  
12 that during a dry period, the atmospheric CO<sub>2</sub> flux consumed through rock weathering was lower  
13  
14 than that during a more humid period. However, middle-latitude and subtropical larger rivers have  
15  
16 high bicarbonate (HCO<sub>3</sub><sup>-</sup>) concentrations and fluxes because of the abundant distribution of  
17  
18 carbonate minerals in their drainage basins. In contrast, tropical larger rivers, such as the Amazon  
19  
20 and Orinoco Rivers, have low HCO<sub>3</sub><sup>-</sup> concentrations (Cai et al., 2010).

21  
22  
23 Large rivers also generate offshore plumes that are characterized by high buoyancy and biological  
24  
25 productivity because of their low salinities, high levels of nutrients, and suspended and dissolved  
26  
27 terrestrial materials (Higgins et al., 2006; Kouamé et al., 2009; Kang et al., 2013). As a result, the  
28  
29 chemical, geological, biological and physical environments of the adjacent marginal seas are  
30  
31 affected. Low-salinity regions at the eastern edge (SSS <35) in the Atlantic Ocean can be found in  
32  
33 two regions according to Bakker et al. (1999): one north of the equator and one near the Congo  
34  
35 River. Van Bennekom et al. (1978) and Vangriesheim et al. (2009) showed that the influence of  
36  
37 the Congo River ranges from -3.5° to -6.5° latitude and reaches 6.5° E in the Atlantic Ocean (700  
38  
39 km offshore).

40  
41 In the Atlantic Ocean, the dispersal of the Amazon River water leads to a brackish water plume  
42  
43 that can exceed 10<sup>6</sup> km<sup>2</sup>, reaching latitudes as far from the river mouth as 30°W (Coles et al., 2013)  
44  
45 or even 25°W when the North Equatorial Countercurrent (NECC) is strong (Lefèvre et al., 1998).  
46  
47 Recently, Ibánhez et al. (2017) compared the monthly precipitation rate with the monthly SSS in  
48  
49 five regions of the tropical Atlantic. They found highly significant linear relationships of  
50  
51  
52  
53  
54  
55  
56  
57  
58  
59  
60  
61  
62  
63  
64  
65

1  
2  
3  
4 precipitation with SSS across the western Atlantic basin. The extension of the Amazon River plume  
5  
6 was highly significant, ranging from 0.25 to  $1.60 \times 10^6 \text{ km}^2$ , after removing the influence of rainfall.  
7  
8  
9 In Tropical Atlantic regions, low salinity patches are related to large rivers, such as the Amazon  
10  
11 ( $5413 \text{ km}^3 \text{ year}^{-1}$ ), followed by the Congo ( $1263 \text{ km}^3 \text{ year}^{-1}$ ) and Orinoco ( $1170 \text{ km}^3 \text{ year}^{-1}$ ),  
12  
13 spreading freshwater by surface oceanic circulation (Araujo et al. 2014).  
14

15  
16 According to Araujo et al. (2014), significant differences were observed between the large  
17  
18 estuarine systems of the Atlantic Ocean. The authors indicated that  $C_T$  and TA showed significant  
19  
20 differences between the eastern (Volta, Niger and Congo Rivers) and western (Orinoco, Amazon,  
21  
22 São Francisco and Paraíba do Sul Rivers) estuaries. Other important parameters also showed  
23  
24 significant differences, such as  $p\text{CO}_2$  and dissolved organic carbon (DOC). According to these  
25  
26 authors, DOC is higher in the eastern region; this would affect coastal concentrations in that region,  
27  
28 increasing  $C_T$  levels in the adjacent coastal region. Additionally, TA is mainly affected by the  
29  
30 chemical reactions of the different types of rocks in the soils of the hydrographic basins, which are  
31  
32 carried to the coastal region via runoff  
33  
34  
35  
36  
37

38  
39 Based on the approaches of Ternon et al. (2000), Körtzinger (2003), Cooley and Yager (2006) and  
40  
41 Araujo et al. (2014), a simple conservative mixing model was used to calculate the proportions of  
42  
43  $C_T$  in western rivers (Amazon and Orinoco) and eastern rivers (Niger, Volta and Congo) for plume  
44  
45 water and seawater in a given plume sample (Figure 10). This mixing model approach has been  
46  
47 widely detailed in the supplementary material of Araujo et al. (2014). It is assumed that the effects  
48  
49 of precipitation and evaporation on the carbon and freshwater mass balances are small compared  
50  
51 to the river (Cooley and Yager, 2006) over the first 10 m-deep plume. Additional variations in  $C_T$   
52  
53 not attributable to mixing were then ascribed to biology ( $C_{T\text{bio}}$ ). Using the mixing equations of  
54  
55 Araujo et al. (2014), we used TA, SSS and  $C_T$  to estimate the excess or deficit of  $C_{T\text{bio}}$  in the east  
56  
57 and west coastal regions ( $T_{\text{Abio}}$  calculation is not necessary here, as TA is considered a  
58  
59  
60  
61  
62  
63  
64  
65

1  
2  
3  
4 conservative parameter). Positive values of  $\Delta CT_{bio}$  indicate an inorganic carbon deficit, implying  
5  
6 that the respiration process exceeds the respiration process. Thus, the system is considered to be  
7  
8 autotrophic, while negative CT values indicate excess CT, suggesting that respiration > production,  
9  
10 and the system is considered heterotrophic. The results showed that both regions had negative  
11  
12  $CT_{bio}$  values in the estuarine region, indicative of excess CT. Outside the plume, the values  
13  
14 oscillate between positive and negative; however, the mean values of the gradients indicate excess  
15  
16 CT. In the western region, 7% of the CT excess (bio) average across the entire saline gradient was  
17  
18 obtained, while in the eastern region, this percentage was lower (0.2%). According to these results,  
19  
20 the primary productivity in the eastern region is higher than that in the western region (Figure 10 a  
21  
22 and b). Additionally, we have to consider that the extension of the plumes differs, and the saline  
23  
24 values are smaller in the western region, generating a greater amplitude of variation between the  
25  
26 CT values. The concentrations of  $HCO_3^-$  (the main component of CT coming from the rocks) in  
27  
28 the eastern region are higher; however, the freshwater flow is greater in the western region. The  
29  
30 observed concentrations showed that the western region has an average  $CT_{bio}$  excess of  $92 \mu mol$   
31  
32  $kg^{-1}$ , while the eastern region has an average  $CT_{bio}$  excess of  $3 \mu mol kg^{-1}$ . In estuarine zones, these  
33  
34 excesses of CT are greater. In the western region, it reached 14%, while in the estuarine zone of  
35  
36 the eastern region, it was 1%.

#### 4.4. Regional differences in carbonate chemistry

47  
48 The ratio of TA to the dissolved inorganic carbon concentration (TA: $C_T$ ) is of particular interest  
49  
50 because it serves as an indicator of the relative abundance of carbonate species (e.g.,  $HCO_3^-$  and  
51  
52  $CO_3^{2-}$ ) in seawater. According to Wang et al. (2013), for a specific temperature and pressure, the  
53  
54  $CO_2$  system parameters, such as the aragonite saturation state and pH value, are closely correlated  
55  
56  
57  
58  
59  
60  
61  
62  
63  
64  
65

1  
2  
3  
4 with this ratio, which has been widely used in studies of seawater carbonate chemistry (Zeebe and  
5  
6  
7 Wolf-Gladrow, 2001).

8  
9 Differences in the seawater TA:  $C_T$  imply, for example, differences in buffer intensity, also called  
10  
11 buffer capacity (Revelle factor). The buffer intensity of the seawater carbonate system is at a  
12  
13 minimum when  $CO_3^{2-} \sim CO_{2aq}$ , where the TA and  $C_T$  concentrations are approximately equal (i.e.,  
14  
15 when TA:  $C_T \approx 1$ ).

16  
17  
18 In **Figure 8** (corresponding to the NW region), water with a relatively low salinity (<35) dominates.  
19  
20 A linear regression line derived from the SSS=20-37 portion of the TA-SSS plot produced a very  
21  
22 low TA. In contrast, in **Figure 8C** (SW region), high SSS values (>32) are observed in the TA-  
23  
24 SSS plot. This region is not affected by major river discharge. The variations in TA and SSS are  
25  
26 assigned to physical factors, especially the balance between precipitation and evaporation.  
27  
28

29  
30 The eastern edge (**Figure 8B** and **Figure 8D**) has regions with high productivity associated with  
31  
32 the discharge of large rivers, such as the Niger and Congo Rivers. In **Figure 8B**, a very low TA  
33  
34 was observed at zero salinity. As indicated in Section 3.5, low rates of  $CO_2$  consumption have been  
35  
36 reported for the Niger and Congo Rivers. As a result, the chemical, geological, biological and  
37  
38 physical environments of coastal areas are affected. Low-salinity regions at the eastern edge (SSS  
39  
40 <35) in the Atlantic Ocean can be found in two regions according to Bakker et al. (1999): one north  
41  
42 of the equator and one near the Congo River. In contrast, in high-salinity offshore waters (>32),  
43  
44 TA and SSS exhibited a tight linear correlation with an elevated TA.  
45  
46  
47

48  
49 The in-situ observations of TA and  $C_T$  obtained in the coastal regions of Africa and Brazil show  
50  
51 significant differences (Bonou et al., 2016b). The biogeochemical composition of each border is  
52  
53 different, and many different processes occur at each border, which are different from one another,  
54  
55 including in the  $SSS \geq 35$  regions.  
56  
57  
58  
59  
60  
61  
62  
63  
64  
65

1  
2  
3  
4 **Figure 8**  
5  
6  
7

8  
9 The values observed here showed typical values for tropical waters, with a slight increase in the  
10 average values in the TA:CT (SW region; **Figure 9C**).  
11  
12

13  
14 **Figure 9B** to **Figure 9D** show a relatively well-buffered TA:  $C_T > 1.15$ , while **Figure 9A** indicates  
15 a minor buffering capacity (TA: $C_T = 1.1$ ). A lower buffer capacity may respond to coastal  
16 acidification, such as increases in atmospheric CO<sub>2</sub> or eutrophication events.  
17  
18

19 Biogeochemical processes such as photosynthesis, respiration (P-R), and air–sea CO<sub>2</sub> exchange  
20 also change the  $C_T$ . Changes in the  $C_T$  in regions with high fluvial discharge can alter these  
21 processes and consequently reduce the TA: $C_T$  ratio. In the SW region, TA: $C_T$  is high, making  
22 conditions more favorable for oceanic uptake of atmospheric CO<sub>2</sub>.  
23  
24  
25  
26  
27  
28  
29  
30  
31  
32

33 **Figure 9**  
34  
35  
36  
37

38 **5. Conclusions**  
39

40 The tropical Atlantic Ocean receives an important amount of carbon from the African and South  
41 American continents, which present different features at their oceanic borders. In this work, the  
42 comparative study of TA and  $C_T$  data from the coastal region of Africa and Brazil shows significant  
43 differences between these variables (Mann–Whitney test,  $\alpha=0.05$ ,  $p=0.0001$ ). These differences  
44 are explained by the differences in biological activities, the influence of rivers, and the composition  
45 of biogeochemicals in different coastal areas. At the western tropical border, the minimum values  
46 of the carbon parameters were obtained, while higher values of the carbon parameters were  
47 obtained in the eastern tropical Atlantic border. The biogeochemical composition of each border is  
48 different, and many different processes occur at each border. The coastal upwelling process at the  
49  
50  
51  
52  
53  
54  
55  
56  
57  
58  
59  
60  
61  
62  
63  
64  
65

1  
2  
3  
4 eastern border contributes to the higher CO<sub>2</sub> concentrations obtained in the eastern coastal area  
5  
6 compared to those obtained at the western edge. This physical process increases the CO<sub>2</sub>  
7  
8 parameters in surface water, followed by an additional physical process that transports the rich  
9  
10 water masses from the African coast to the Brazilian coast through oceanic circulation (SEC). The  
11  
12 river characteristics at each border are different in terms of their physical and biological activities  
13  
14 and chemical composition. The existing TA and C<sub>T</sub> relationships present spatial limitations, and  
15  
16 the use of the empirical TA relationship determined by Lefèvre et al. (2010) for the observation  
17  
18 data at the eastern border presents high root mean square error values. The similarity between the  
19  
20 relationships from Takahashi et al. (2014) and Lefèvre et al. (2010) suggests that calculation of the  
21  
22 carbon parameters in the eastern region, using one of these relationships, will lead to a higher root  
23  
24 mean square error value. Otherwise, the climatological map determined by Takahashi et al. (2014)  
25  
26 in the eastern region using this relationship may be affected by an important bias compared to that  
27  
28 in other regions. On the other hand, the TA relationship determined by Koffi et al. (2010) is not a  
29  
30 better relationship to be applied to the coastal data in the Amazon plume. However, we found that  
31  
32 their relationship with TA can be extended to the southwestern part, mainly in the SEC region, for  
33  
34 data with SSS<sub>≥</sub>37.  
35  
36  
37  
38  
39  
40  
41  
42

43 In coastal regions, the biogeochemical composition of each border is different, and many different  
44  
45 processes occur at each border, principally regions that include values for SSS<sub><</sub>35.  
46  
47  
48  
49

### 50 **Author contributions**

51  
52 All authors contributed extensively to the interpretation of the results and to the writing of the  
53  
54 manuscript.  
55  
56  
57  
58  
59  
60  
61  
62  
63  
64  
65

1  
2  
3  
4 **Acknowledgments**  
5

6 We are grateful to the SNAPO-CO<sub>2</sub> (Service National d'Analyses des Paramètres du CO<sub>2</sub>) at  
7 LOCEAN (Paris) for the TA and C<sub>T</sub> analyses from Plumand, Amandes, PIRATA, Colibri, Aramis,  
8 Rio Blanco, Camadas Finas and Bioamazon cruises. We acknowledge the scientific and crew  
9 members of the NOc. Antares and NO Antea for their help at sea and to the Marine Nantaise and  
10 Hamburg Sud for allowing sampling onboard their merchant ships. We thank IRD for the financial  
11 support and the financial contributions from INCT AmbTropic, CNPq/FAPESB (Grants  
12 565054/2010-4 and 8936/2011), LEFE CYBER program, AIRD-FAPEMA BIOAMAZON  
13 project, and the EU integrated project CARBOCHANGE (Grant 264879). F. Bonou acknowledges  
14 Yves du Penhoat, Alexis Chaigneau and IRD, and JEAJ for their technical support. C. Noriega  
15 acknowledges the National Council for Scientific and Technological Development – CNPq  
16 (Project 465634/2014-1; process number 370821/2019-0; INCT program). This work is a  
17 contribution of the Brazilian Research Network on Global Climate Change, Rede CLIMA  
18 (<http://redeclima.ccst.inpe.br/>).  
19  
20  
21  
22  
23  
24  
25  
26  
27  
28  
29  
30  
31  
32  
33  
34  
35  
36  
37  
38  
39  
40  
41

42 **Conflict of Interest Statement:** The authors declare that the research was conducted in the absence  
43 of any commercial or financial relationships that could be construed as a potential conflict of  
44 interest.  
45  
46  
47  
48  
49  
50  
51  
52  
53  
54  
55  
56  
57  
58  
59  
60  
61  
62  
63  
64  
65

1  
2  
3  
4 **List of figures**  
5  
6  
7

8  
9 **Figure 1.** Routes of the different cruises (55 cruises), indicating the geographical positions of the  
10 total alkalinity (TA) samples in the Tropical Atlantic. The red and green colors represent samples  
11 collected from the western and eastern tropical Atlantic, respectively, with  $SSS < 35$ , and the black  
12 points are data with  $SSS \geq 35$  in the tropical Atlantic.  
13  
14

15  
16  
17  
18 **Figure 2.** Standard deviation of SSS anomalies for the period from 1970-2013, showing the  
19 coastal regions with greater variability in SSS under the influence of rivers.  
20  
21

22  
23  
24 **Figure 3.** Monthly distribution of SST ( $^{\circ}\text{C}$ ) for January and July during the period of 1958-2014  
25 in the tropical Atlantic.  
26  
27

28  
29 **Figure 4.** SST climatology of the western and eastern regions for the 1958-2014 period (OAFlux  
30 database - <http://oaflux.whoi.edu/>). NW ( $-70^{\circ}\text{W}$  to  $-35^{\circ}\text{W}$ ;  $0^{\circ}$  to  $20^{\circ}\text{N}$ ); NE ( $-35^{\circ}\text{W}$  to  $+10^{\circ}\text{W}$ ;  $0^{\circ}$   
31 to  $20^{\circ}\text{N}$ ); SW ( $-50^{\circ}\text{W}$  to  $-15^{\circ}\text{W}$ ;  $0^{\circ}$  to  $-20^{\circ}\text{S}$ ); SE ( $-15^{\circ}\text{W}$  to  $+10^{\circ}\text{W}$ ;  $0^{\circ}$  to  $-20^{\circ}\text{S}$ ).  
32  
33  
34

35  
36 **Figure 5.** Comparisons among **A)** empirical relationships of Koffi et al. (2010) and Lefèvre et al.  
37 (2010) for the estimated TA applied to data with  $SSS < 35$  in the western tropical Atlantic; **B)**  
38 empirical relationships of Koffi et al. (2010) and Lefèvre et al. (2010) for the estimated TA  
39 applied to data with  $SSS < 35$  in the eastern tropical Atlantic; **C)** empirical relationships of Koffi  
40 et al. (2010) and Lefèvre et al. (2010) for the estimated TA applied to data with  $SSS \geq 35$  in the  
41 central tropical Atlantic.  
42  
43  
44  
45  
46  
47

48  
49 **Figure 6.** Localization of data with  $SSS \geq 37$  around Koffi et al. (2010) lines in green and of data  
50 with  $SSS \geq 35$  in black in the central region of the tropical Atlantic.  
51  
52  
53

54  
55 **Figure 7.** Annual average data from 10 years (2006-2015) of the chlorophyll-*a* concentrations in  
56 the tropical Atlantic Ocean (MODIS-Aqua; 4 km resolution), obtained from  
57 <https://giovanni.gsfc.nasa.gov/giovanni/>. (Data access: 2017.05.09).  
58  
59  
60



1  
2  
3  
4 **Figure 8:** TA-SSS relationship in the different subregions in the Atlantic Ocean.  
5  
6

7  
8 **Figure 9:** TA:C<sub>T</sub> for the NW region (A); NE region (B); SW region (C) and SE region (D). The  
9  
10 black line TA:C<sub>T</sub> =1; the dashed line indicates the tendency of the observed values. 4.7. C<sub>T</sub> and  
11  
12 TA normalization in the tropical Atlantic.  
13  
14

15  
16  
17 **Figure 10:** C<sub>T</sub> bio (C<sub>T<sub>excess</sub></sub>) derived from the mixing model in function SSS (a) in the western  
18  
19 region and (b) in the eastern region  
20  
21  
22  
23  
24  
25  
26  
27  
28  
29  
30  
31

## 32 Tables

33  
34  
35  
36  
37

38 **Table 1.** Empirical carbon relationships available for the regions near tropical Atlantic Rivers.  
39

REGION	EMPIRICAL RELATION	REFERENCE
Western	TA = 58 * SSS+265	Lefèvre et al. (2010)
	C <sub>T</sub> = 50.1*SSS+0.9*(Year-1989) +198	Bonou et al. (2016a)
Eastern	TA = 65.52*SSS+2.50	Koffi et al. (2010)
	C <sub>T</sub> = 51.71*SSS-12.79*SST +507.82	Koffi et al. (2010)
Tropical Atlantic	TA = 58.25*SSS+270.9	Takahashi et al. (2014a)

40  
41  
42  
43  
44  
45  
46  
47  
48  
49  
50  
51  
52  
53  
54  
55  
56  
57  
58  
59  
60  
61  
62  
63  
64  
65

**Table 2.** Additional data cruises used in this paper with measurements of TA and C<sub>T</sub> compiled with data from Bonou et al. (2016) for all tropical Atlantic Ocean data.

CRUISE	PERIOD	SHIP	REFERENCE	METHODOLOGY		PRECISION/ ACCURACY	
				TA <sup>a</sup>	C <sub>T</sub>	TA (μmol kg <sup>-1</sup> )	C <sub>T</sub> (μmol kg <sup>-1</sup> )
TTOTASSV	Dec 1982- Jan 1983	<i>R/V Knorr</i>	Takahashi et al.(2014b)	-	-	-	-
AJAX_1983	Oct 1983- Fev 1984	<i>R/V Knorr</i>	Chipman et al. (2007)	-	-	-	-
SAVE-1	Nov-1987	<i>R/V Knorr</i>	Takahashi et al. (1995)	-	-	-	-
SAVE-2	Dec-1987	<i>R/V Knorr</i>	Takahashi et al. (1995)	-	-	-	-
SAVE-3	Jan-1988	<i>R/V Knorr</i>	Takahashi et al. (1995)	-	-	-	-
WOCE-A16C (SAVE)	Mar-Apr 1989	<i>R/V Melville</i>	Takahashi et al. (1989)	-	-	±2/±2	±2/±2
CITHER 1	Jan- Mar 1993	<i>R/V Atalante</i>	Oudot et al. (1995)	-	Chromatography	-	-
EGEE-1	Jun-Jul 2005	<i>R/V Antea</i>	Koffi et al. (2010)	Full	-	±2/±2	±2/±2
EGEE-2	Sep 2005	<i>R/V Antea</i>	Koffi et al. (2010)	Full	-	-	-
EGEE-3	Mai-Sep 2006	<i>R/V Antea</i>	Koffi et al. (2010)	Full	-	-	-
EGEE-5	Jun-Jul 2007	<i>R/V Antea</i>	Koffi et al. (2010)	Full	-	-	-
EGEE-5	Jun-Jul 2007	<i>R/V Antea</i>	Koffi et al. (2010)	Full	-	-	-
EGEE-6	Set 2007	<i>R/V Antea</i>	Koffi et al. (2010)	Full	-	-	-
CITHER 2-1	Jan-Mar 1994	<i>R/V Maurice Ewing</i>	Rios et al. (2005)	-	SOMMA	±1.2/±1.2	±1.64/±1.6
WOCE-A15	Abr-May 1994	<i>R/V Knorr</i>	Goyet et al. (1995)	Full	Colorimetry	-	-
METEOR 68/3	Jul-Aug 2006	<i>R/V Meteor</i>	Körtzinger & Steinhoff (2012)	Full	SOMMA	-	-
AMT7	Set-Oct 1998	<i>RRS James Clark Ross</i>	Lefèvre et al. (2002)	-	SOMMA	-	-
METEOR 80/1	Oct-Nov 2009	<i>R/V Meteor</i>	Körtzinger et al. (2012)	Full	SOMMA	-	-
FICARAM_X V	Mar-May 2013	<i>Hisperides</i>	Perez et al. (2013)	Full	-	-	-
CARINA.ATL	1999-2004	<i>Various ships</i>	This Study	Full	Potentiometry	-	-

<sup>a</sup>Determined by potentiometric titration, either a full curve (“Full”) or a single-point (“1-point”) titration. No TA was measured during the AMT7 cruise.

14  
15  
16  
17  
18  
19  
20  
21  
22  
23  
24  
25  
26  
27  
28  
29  
30  
31  
32  
33  
34  
35  
36  
37  
38  
39  
40  
41  
42  
43  
44  
45  
46  
47  
48  
49  
50  
51  
52  
53  
54  
55  
56  
57  
58  
59  
60  
61  
62  
63  
64  
65

**Table 3.** Descriptive statistics (minimum as min, maximum as max, mean and standard deviation as STD) of TA and C<sub>T</sub> in the eastern region (103 data points) and western region (392 data points).

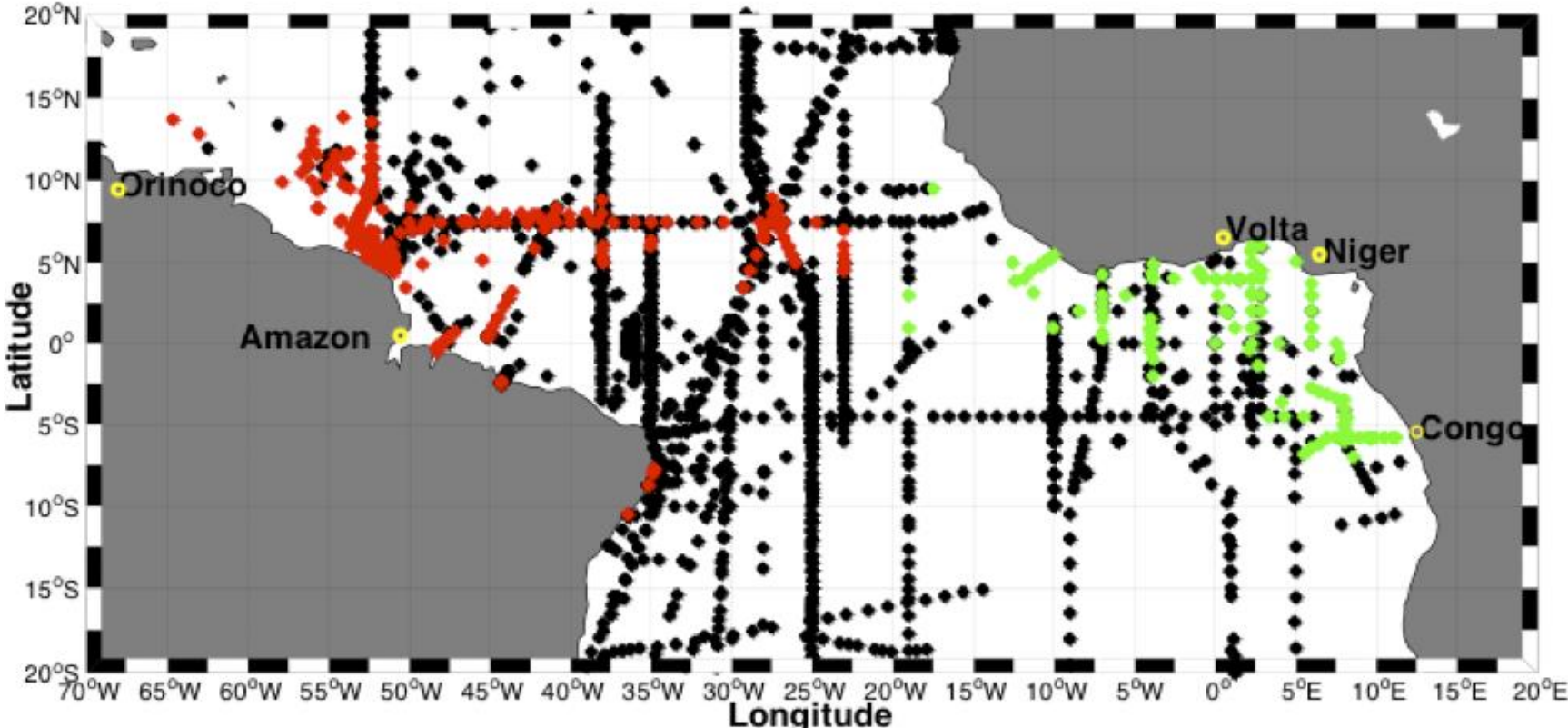
REGION	TA (μmol kg <sup>-1</sup> )				C <sub>T</sub> (μmol kg <sup>-1</sup> )				SSS			SST(°C)				
	Min	Max	Mean	STD	Min	Max	Mean	STD	Max	Min	Mean	STD	Max	Min	Mean	STD
Western	323.0	2372.0	2099.4	286.4	397.7	2075.3	1779.6	236.4	34.9	1.1	31.	4.9	30.5	25.5	28.6	0.8
Eastern	1492.9	2320.7	2198.0	141.9	1389.6	2033.0	1892.2	94.2	34.9	22.9	33.6	2.1	29.1	22.8	27.8	1.2

**Table 4.** Root mean square error (rmse) of estimated TA and C<sub>T</sub> from existing relationships.

PARAMETER	REGION	N	REFERENCE	RMSE (μmol kg <sup>-1</sup> )
TA	Western (SSS<35)	392	Lefèvre et al. (2010)	28.6
			Koffi et al. (2010)	64.8
	Eastern (SSS<35)	103	Lefèvre et al. (2010)	28.5
			Koffi et al. (2010)	12.5
	Central (SSS≥35)	1848	Lefèvre et al. (2010)	20.5
			Koffi et al. (2010)	19.2
C <sub>T</sub>	Western (SSS<35)	392	Bonou et al. (2016a)	41.1
			Koffi et al. (2010)	47.9
	Eastern (SSS<35)	103	Bonou et al. (2016a)	29.6
			Koffi et al. (2010)	28.1
	Central (SSS≥35)	1848	Bonou et al. (2016a)	35.1
			Koffi et al. (2010)	34.7

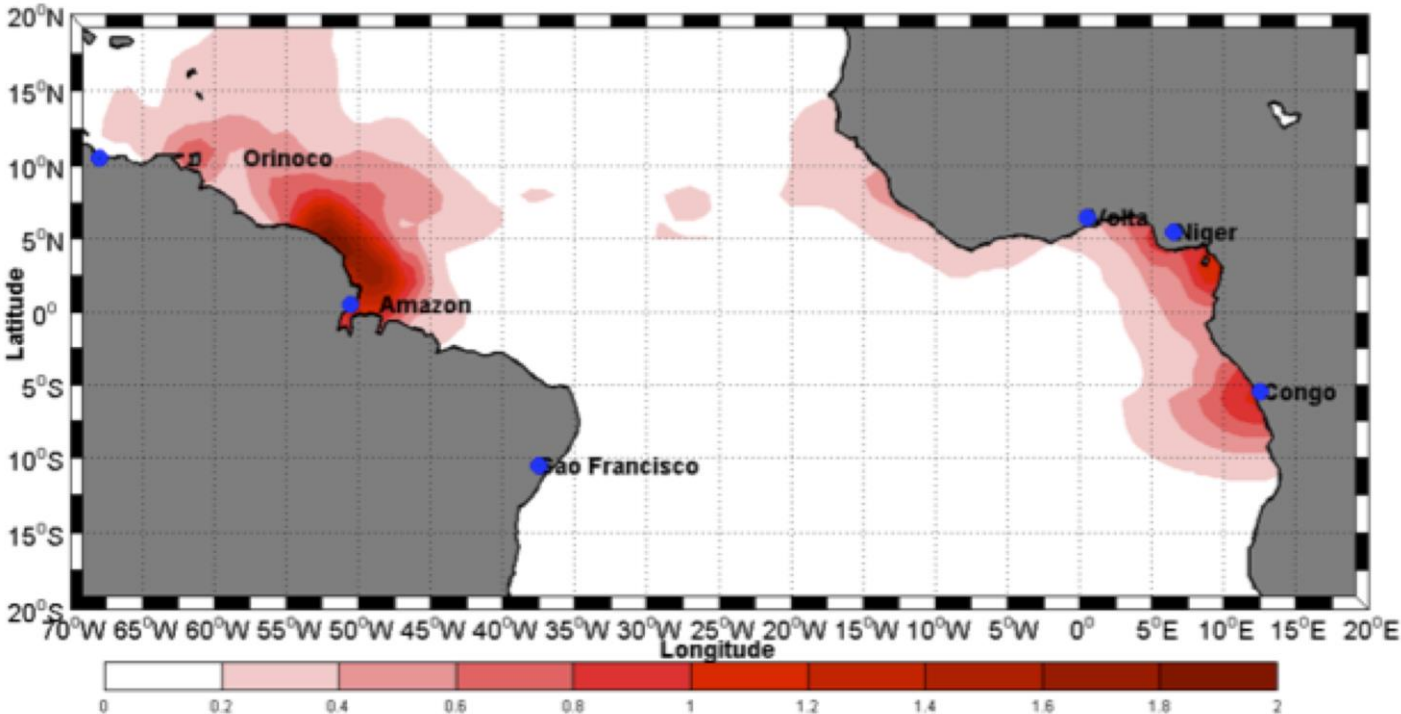
14  
15  
16  
17  
18  
19  
20  
21  
22  
23  
24  
25  
26  
27  
28  
29  
30  
31  
32  
33  
34  
35  
36  
37  
38  
39  
40  
41  
42  
43  
44  
45  
46  
47  
48  
49  
50  
51  
52  
53  
54  
55  
56  
57  
58  
59  
60  
61  
62  
63  
64  
65

Figure 1



14  
15  
16  
17  
18  
19  
20  
21  
22  
23  
24  
25  
26  
27  
28  
29  
30  
31  
32  
33  
34  
35  
36  
37  
38  
39  
40  
41  
42  
43  
44  
45  
46  
47  
48  
49  
50  
51  
52  
53  
54  
55  
56  
57  
58  
59  
60  
61  
62  
63  
64  
65

Figure 2



14  
15  
16  
17  
18  
19  
20  
21  
22  
23  
24  
25  
26  
27  
28  
29  
30  
31  
32  
33  
34  
35  
36  
37  
38  
39  
40  
41  
42  
43  
44  
45  
46  
47  
48  
49  
50  
51  
52  
53  
54  
55  
56  
57  
58  
59  
60  
61  
62  
63  
64  
65

Figure 3

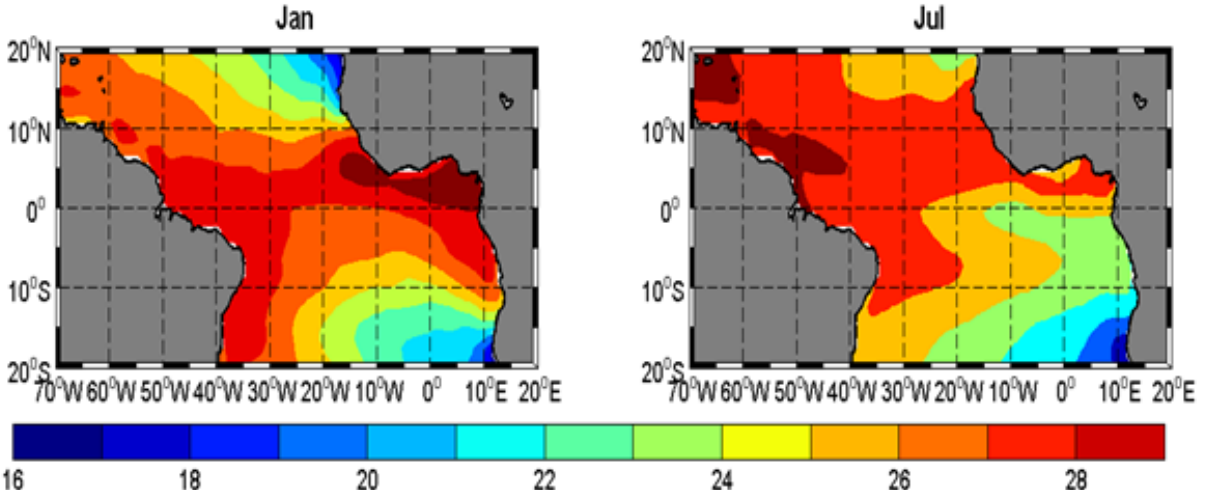
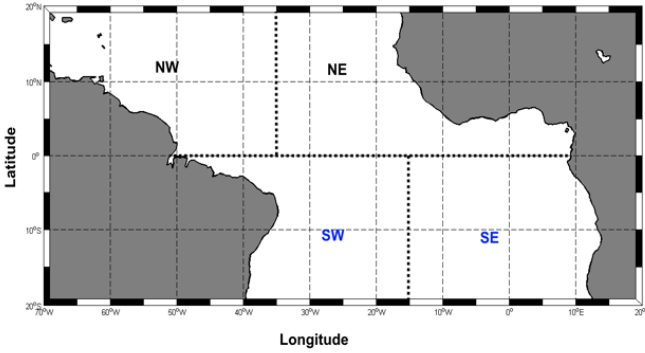
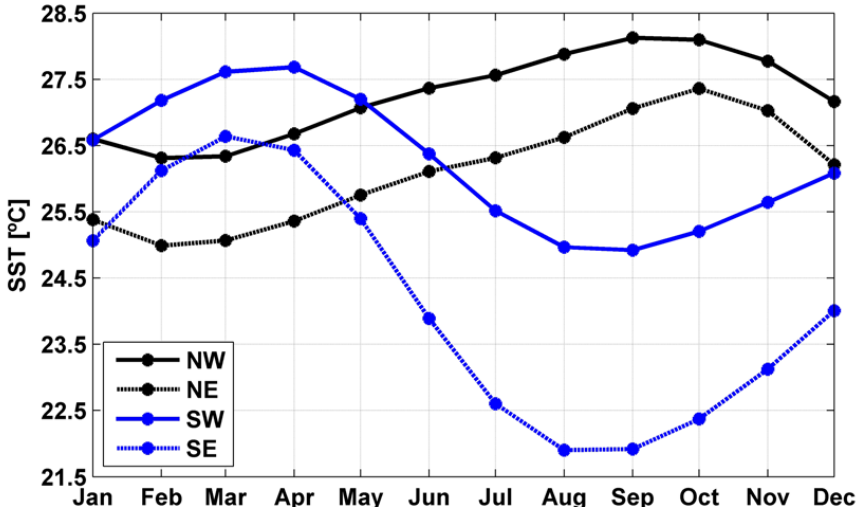
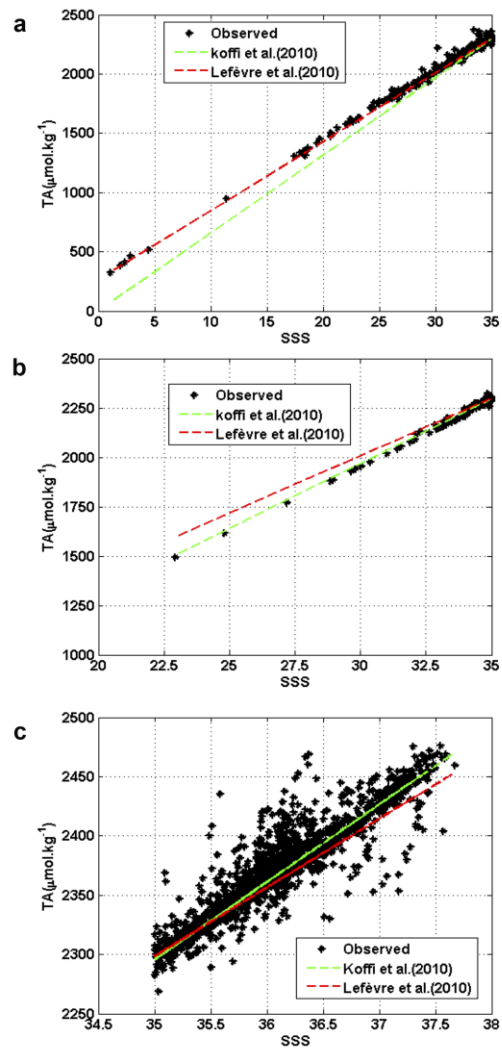


Figure 4



14  
15  
16  
17  
18  
19  
20  
21  
22  
23  
24  
25  
26  
27  
28  
29  
30  
31  
32  
33  
34  
35  
36  
37  
38  
39  
40  
41  
42  
43  
44  
45  
46  
47  
48  
49  
50  
51  
52  
53  
54  
55  
56  
57  
58  
59  
60  
61  
62  
63  
64  
65

Figure 5



14  
15  
16  
17  
18  
19  
20  
21  
22  
23  
24  
25  
26  
27  
28  
29  
30  
31  
32  
33  
34  
35  
36  
37  
38  
39  
40  
41  
42  
43  
44  
45  
46  
47  
48  
49  
50  
51  
52  
53  
54  
55  
56  
57  
58  
59  
60  
61  
62  
63  
64  
65

Figure 6

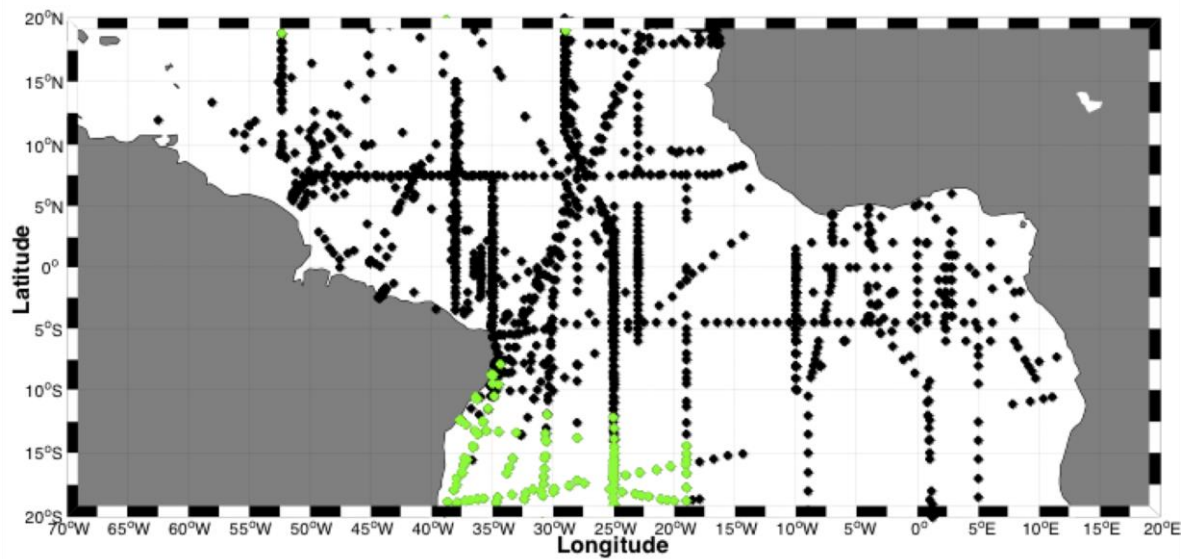
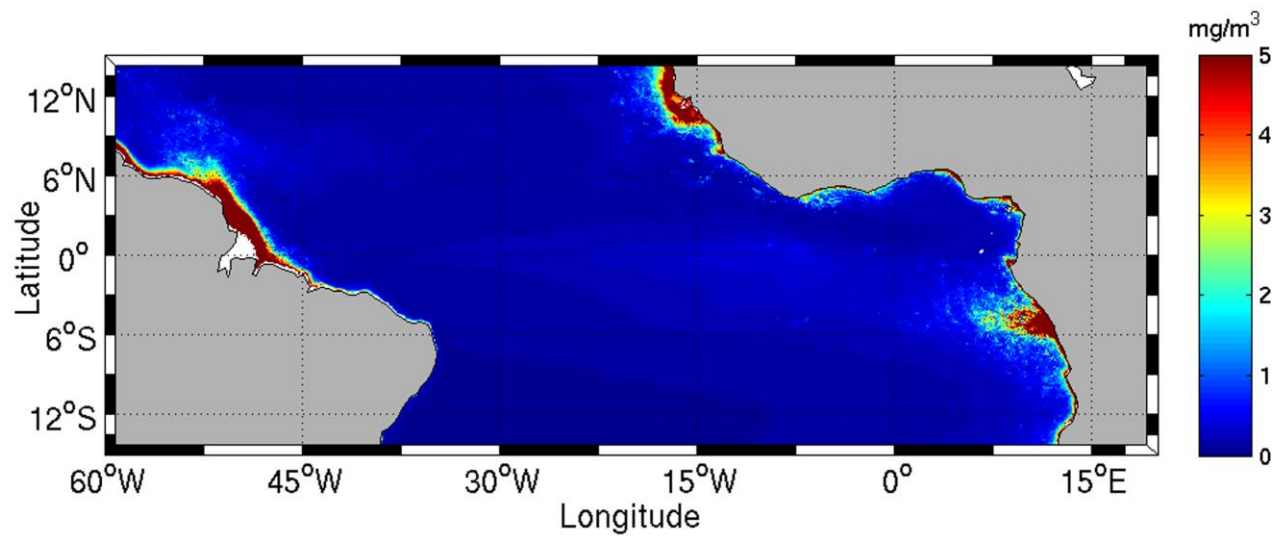


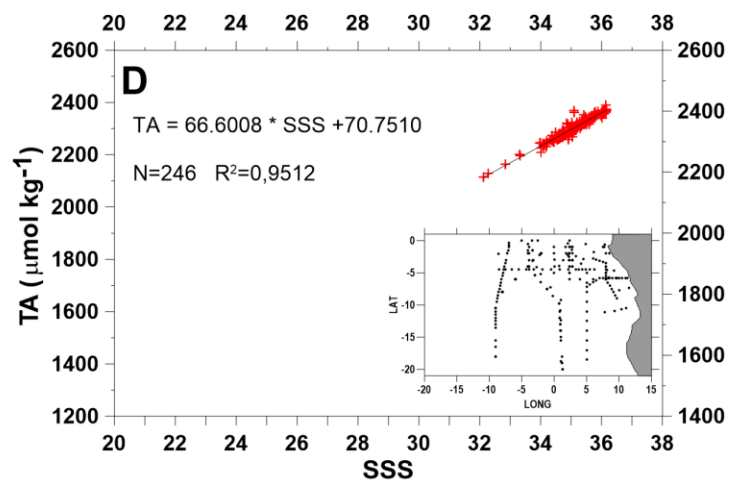
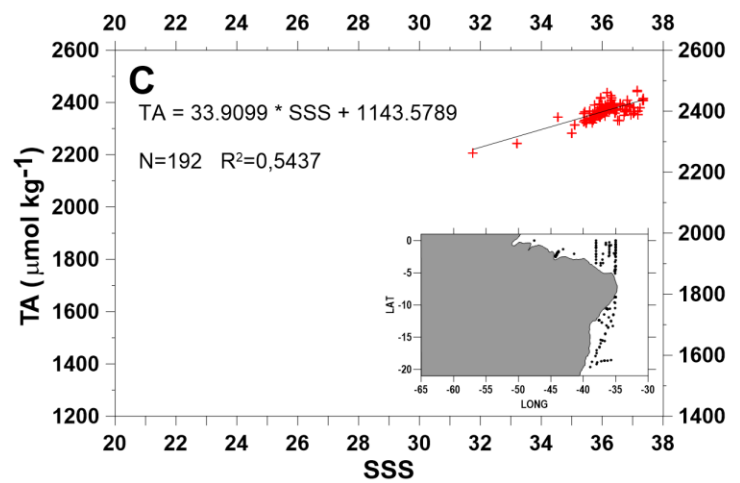
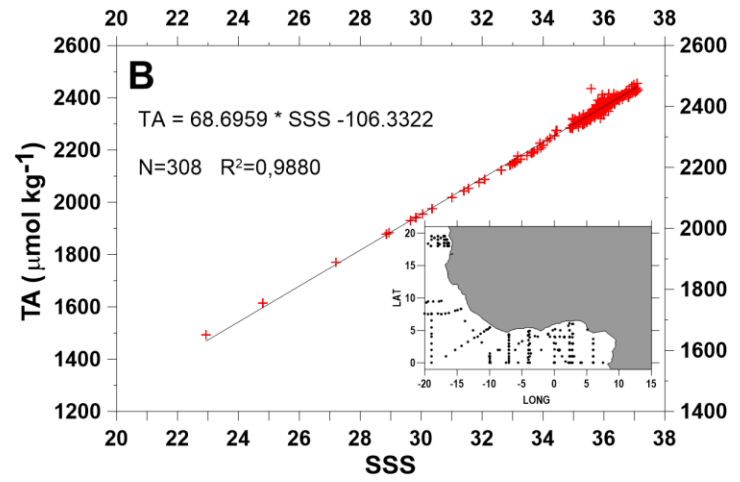
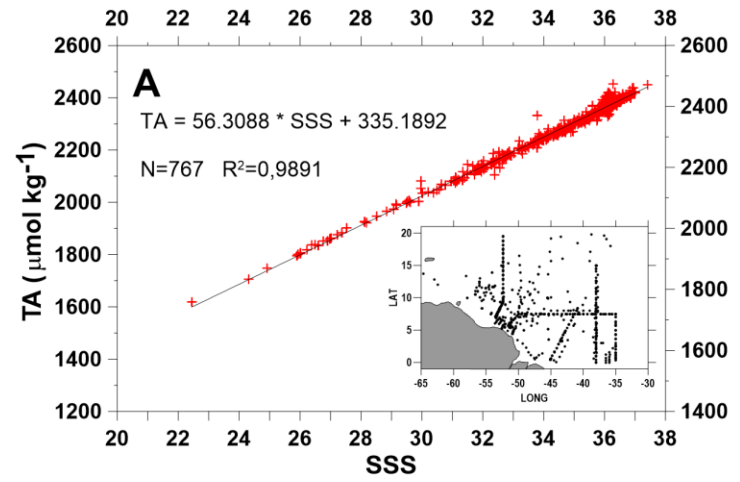
Figure 7





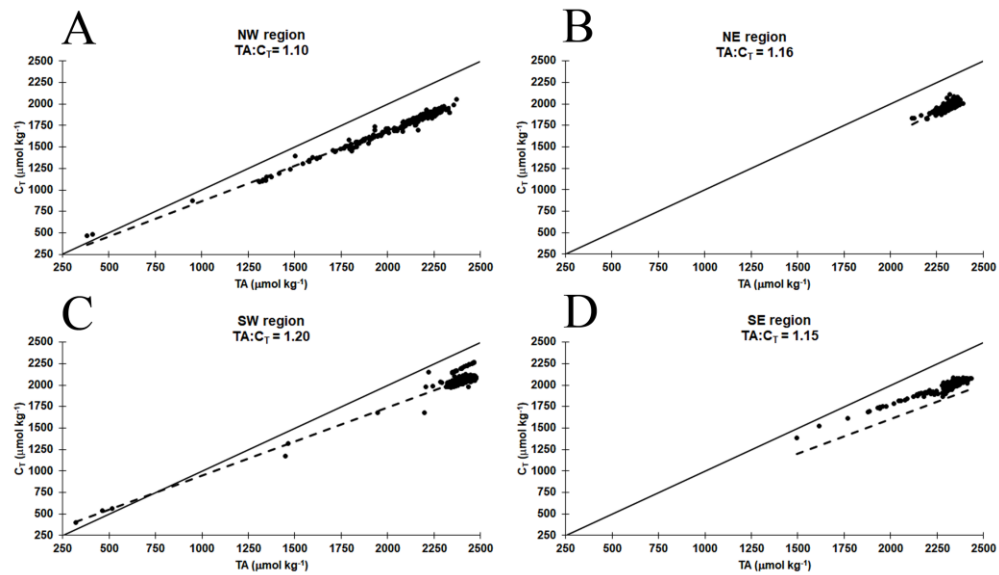
14  
15  
16  
17  
18  
19  
20  
21  
22  
23  
24  
25  
26  
27  
28  
29  
30  
31  
32  
33  
34  
35  
36  
37  
38  
39  
40  
41  
42  
43  
44  
45  
46  
47  
48  
49  
50  
51  
52  
53  
54  
55  
56  
57  
58  
59  
60  
61  
62  
63  
64  
65

Figure 8



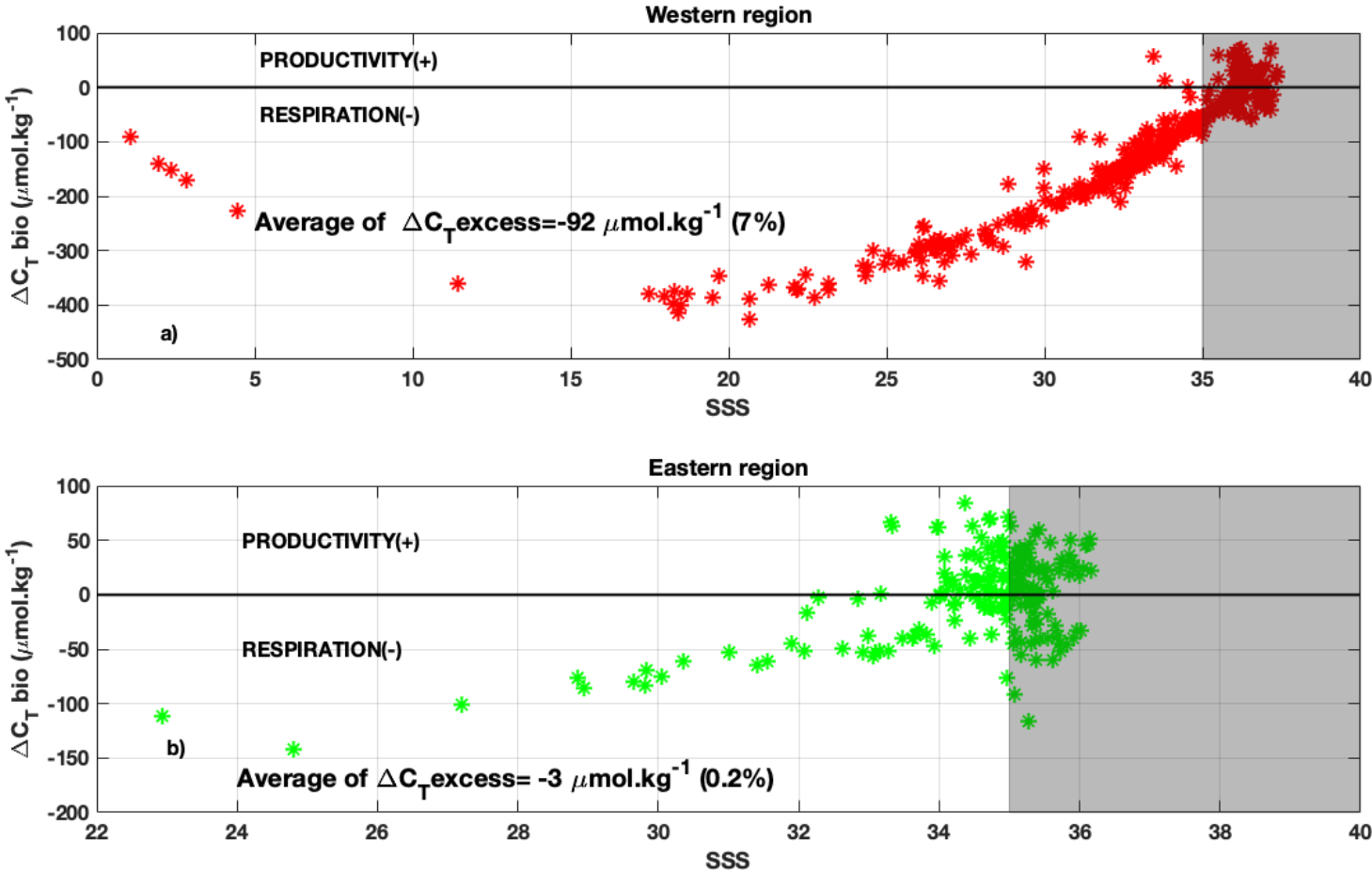
14  
15  
16  
17  
18  
19  
20  
21  
22  
23  
24  
25  
26  
27  
28  
29  
30  
31  
32  
33  
34  
35  
36  
37  
38  
39  
40  
41  
42  
43  
44  
45  
46  
47  
48  
49  
50  
51  
52  
53  
54  
55  
56  
57  
58  
59  
60  
61  
62  
63  
64  
65

Figure 9



14  
15  
16  
17  
18  
19  
20  
21  
22  
23  
24  
25  
26  
27  
28  
29  
30  
31  
32  
33  
34  
35  
36  
37  
38  
39  
40  
41  
42  
43  
44  
45  
46  
47  
48  
49  
50  
51  
52  
53  
54  
55  
56  
57  
58  
59  
60  
61  
62  
63  
64  
65

Figure 10





# Editing Certificate

This document certifies that the manuscript

## **A comparative study of total alkalinity and total inorganic carbon near tropical Atlantic coastal region**

prepared by the authors

**Frédéric Bonou, Carmen Medeiros, Carlos Noriega, Moacyr Araujo, Aubains Hounsou-Gbo and Nathalie Lefèvre**

was edited for proper English language, grammar, punctuation, spelling, and overall style by one or more of the highly qualified native English speaking editors at AJE.

This certificate was issued on **May 26, 2022** and may be verified on the [AJE website](#) using the verification code **C1DE-BDDO-78A5-019D-89DC**.



Neither the research content nor the authors' intentions were altered in any way during the editing process. Documents receiving this certification should be English-ready for publication; however, the author has the ability to accept or reject our suggestions and changes. To verify the final AJE edited version, please visit our verification page at [aje.com/certificate](http://aje.com/certificate). If you have any questions or concerns about this edited document, please contact AJE at [support@aje.com](mailto:support@aje.com).

AJE provides a range of editing, translation, and manuscript services for researchers and publishers around the world.

For more information about our company, services, and partner discounts, please visit [aje.com](http://aje.com).

1  
2  
3  
4  
5  
6  
7  
8  
9  
10  
11  
12  
13  
14  
15  
16  
17  
18  
19  
20  
21  
22  
23  
24  
25  
26  
27  
28  
29  
30  
31  
32  
33  
34  
35  
36  
37  
38  
39  
40  
41  
42  
43  
44  
45  
46  
47  
48  
49  
50  
51  
52  
53  
54  
55  
56  
57  
58  
59  
60  
61  
62  
63  
64  
65

## A comparative study ~~of on~~ total alkalinity and total inorganic carbon near ~~the~~ tropical Atlantic coastal region

### Abstract

This paper is based on a comparison of the carbon parameters at the western and eastern borders of the tropical Atlantic using data collected from 55 cruises. Oceanic and coastal data, mainly total alkalinity (TA), total dissolved inorganic carbon ( $C_T$ ), sea surface salinity (SSS) and sea surface temperature (SST), were compiled from different sources. These data were subdivided into three subsets: oceanic data, coastal data and adjacent to the Brazilian (western) and African coastal areas (eastern) data. Significant differences between the TA data ( $2099.4 \pm 286.4 \mu\text{mol kg}^{-1}$ ) at the western and eastern edges ( $2198 \pm 141.9 \mu\text{mol kg}^{-1}$ ) were observed. Differences in the  $C_T$  values between the western edge ( $1779.6 \pm 236.4 \mu\text{mol kg}^{-1}$ ) and eastern edge ( $1892.2 \pm 94.2 \mu\text{mol kg}^{-1}$ ) were also noted. This pattern was due to the different variabilities ~~of in~~ the carbon parameters between the eastern and western border coastal areas and to the biogeochemistry that drives these parameters. In the western coastal area, the physical features of the continental carbon and oceanic waters mixing ~~through with~~ the freshwater that flows from the Amazon and Orinoco Rivers to the South American coast are different than the physical features of the water that flows from the Congo, Volta and Niger Rivers in the eastern region. Applying the TA empirical relationship to TA with values of  $\text{SSS} < 35$  in the western and eastern ~~region regions~~ leads to a higher root mean square error (rmse) in the eastern and western regions. Therefore, most of the existing TA empirical relationships are most useful at the regional scale due to the difference in the water properties of each region. The relationships of TA and  $C_T$  determined in the western and eastern regions do not reproduce ~~well in-~~ situ data ~~well~~, especially at the adjacent edges. This difference is explained by the difference between the African and Brazilian coasts in terms of their carbon parameter characteristics and processes responsible ~~of for~~ their variation. ~~Basing Based~~ on ~~the~~ mixing model, it has been shown that the primary productivity in the eastern region is higher ~~when compared to that of than that in the~~ western region. This is one of ~~reason that makes the reasons why the~~ carbon parameters ~~are~~ higher in ~~the~~ eastern region. For each region studied, an equation for TA is introduced in this study.

**Commented [A2]:** Your paper was edited for correct English language, grammar, punctuation, and phrasing. In addition, we have made some changes to ensure consistency throughout the paper. These changes are based on our extensive knowledge of what journals typically require. If you would like more details, please contact our Support team.

1  
2  
3  
4  
5  
6  
7  
8  
9  
10  
11  
12  
13  
14  
15  
16  
17  
18  
19  
20  
21  
22  
23  
24  
25  
26  
27  
28  
29  
30  
31  
32  
33  
34  
35  
36  
37  
38  
39  
40  
41  
42  
43  
44  
45  
46  
47  
48  
49  
50  
51  
52  
53  
54  
55  
56  
57  
58  
59  
60  
61  
62  
63  
64  
65

**Keywords:** Carbonate system, Tropical Atlantic, West Africa, Brazilian border, Rivers, Coastal regions, Chemical oceanography.

### Highlights

- ~~Compilation Compiled of~~ three decades of carbon data cruises.
- ~~Investigation Investigated of~~ TA/C<sub>T</sub> differences in tropical Atlantic coastal zones.
- Significant difference between TA/C<sub>T</sub> data from the African and Brazilian coastal areas were determined.
- High influence of C<sub>T</sub> in the eastern region compared to that in the western region of the tropical Atlantic Ocean was recorded.
- Four empirical equations ~~are were~~ proposed for the four regions studied.

### 1. Introduction

~~From Between~~ the African and South American continents, the tropical Atlantic receives approximately 0.1 Pg C yr<sup>-1</sup> of carbon, 0.046 Pg C yr<sup>-1</sup> of dissolved organic carbon (DOC), and 0.053 Pg C yr<sup>-1</sup> of dissolved inorganic carbon total (C<sub>T</sub>) (Huang et al., 2012). ~~According to Araujo et al. (2014),~~ 13.2% of the C<sub>T</sub> and 27.3% of the DOC global values are transported from rivers into the world's oceans. Furthermore, rivers provide 0.8-1.33 Pg C to oceans worldwide, of which ~ 0.53 Pg C is transported from tropical rivers (30°N- 30°S) to adjacent estuarine-coastal systems (Huang et al., 2012).

In the tropical Atlantic, the Amazon River is the ~~first largest major~~ river, flowing from west to east, while the Congo River is the second ~~largest major~~ river, which has a local dynamic in this area (Cai et al., 2008). The ~~transport transport~~ of terrestrial, oceanic and atmospheric carbon in the global carbon cycle ~~are is~~ influenced by rivers. ~~Freshwaters are~~ Freshwater is generally rich in terrestrial and atmospheric carbon and is transported to the ocean through rivers (Araujo et al., 2014). The high nutrient concentrations transported by the river flux within the continental shelf and adjacent

1  
2  
3  
4  
5  
6  
7  
8  
9  
10  
11  
12  
13  
14  
15  
16  
17  
18  
19  
20  
21  
22  
23  
24  
25  
26  
27  
28  
29  
30  
31  
32  
33  
34  
35  
36  
37  
38  
39  
40  
41  
42  
43  
44  
45  
46  
47  
48  
49  
50  
51  
52  
53  
54  
55  
56  
57  
58  
59  
60  
61  
62  
63  
64  
65

oceanic region increase primary production and can lead to the absorption of CO<sub>2</sub> (Körtzinger, 2003; Regnier et al., 2013). Previous studies have also revealed that South American estuaries (western region) and African estuaries (eastern region) are carbon sources (+10.6±7 mmol m<sup>-2</sup> day<sup>-1</sup> and +7.0 mmol m<sup>-2</sup> day<sup>-1</sup>, respectively) for the tropical Atlantic (Araujo et al., 2014). Therefore, the coastal regions adjacent to ~~the~~ rivers are regions with highly variable CO<sub>2</sub> parameters due to the carbon input that occurs through the discharge of rivers into ~~the~~ oceanic regions. The amount of carbon from the continental input at the ~~different-separate~~ edges (eastern and western) can influence the carbonate system, such as the total alkalinity (TA) and total dissolved inorganic carbon (C<sub>T</sub>). It is necessary to collect data at these edges to better understand the variability of these parameters.

Important processes can be responsible for carbonate chemistry changes in the ocean, ~~and~~ they can be described by considering the changes in C<sub>T</sub> and TA. The invasion of CO<sub>2</sub> from (or the release of CO<sub>2</sub> to) the atmosphere increases (or decreases) C<sub>T</sub> while TA remains constant, leading to a rise and drop of [CO<sub>2</sub>], respectively, with opposite changes in pH (since CO<sub>2</sub> is a weak acid). Respiration and photosynthesis ~~lead~~ to the same trends, except that TA ~~changes~~ slightly due to nutrient release and uptake. CaCO<sub>3</sub> precipitation decreases C<sub>T</sub> and TA at a ratio of 1:2 and, counterintuitively, increases [CO<sub>2</sub>], although inorganic carbon is reduced.

The spatial distribution of CO<sub>2</sub> and C<sub>T</sub> in the surface ocean is mainly explained by the temperature-dependent solubility of CO<sub>2</sub> on interannual timescales. Because of increased solubility at low temperatures, warm low-latitude surface water retains less CO<sub>2</sub> (~10 μmol kg<sup>-1</sup>) and C<sub>T</sub> (~2000 μmol kg<sup>-1</sup>) than cold high-latitude surface water (CO<sub>2</sub> ~ 15 mol kg<sup>-1</sup> and C<sub>T</sub> ~ 2100 mol kg<sup>-1</sup>). Significant deviations from these broad trends may occur locally and on seasonal time scales due to changes in salinity and processes such as biological activity, upwelling, temperature variations, river runoff, and other activities that alter C<sub>T</sub> and TA.

1  
2  
3  
4  
5  
6  
7  
8  
9  
10  
11  
12  
13  
14  
15  
16  
17  
18  
19  
20  
21  
22  
23  
24  
25  
26  
27  
28  
29  
30  
31  
32  
33  
34  
35  
36  
37  
38  
39  
40  
41  
42  
43  
44  
45  
46  
47  
48  
49  
50  
51  
52  
53  
54  
55  
56  
57  
58  
59  
60  
61  
62  
63  
64  
65

Some equations have been developed in recent decades to determine the carbon parameters TA, C<sub>T</sub> and fugacity (fCO<sub>2</sub>) as functions of physical and other parameters that are easily measurable and accessible (Takahashi et al., 2014, Lefèvre et al., 2010, Koffi et al., 2010). Linear regression relationships can be a good option to estimate carbon parameters. Empirical equations also present large uncertainties in data due to the complexity of the carbon parameters in coastal areas. Although empirical equations are useful to reproduce carbon parameters, they have spatial and temporal limitations for reproducing carbon parameters well in a whole oceanic basin. There have been few studies that focus ~~in~~ on the tropical Atlantic with an emphasis on the contribution of river discharge to carbon. In 2006, other authors used the relationship TA ~~vs.~~ ~~vs~~-SSS (~~Sea Surface Salinity~~[sea surface salinity](#)) and SST (~~Sea Surface Temperature~~[sea surface temperature](#)) in the tropical Atlantic (30°S-~~30°N~~[30°N](#)) for oceanic regions with the [SSS](#) criterion ~~of SSS~~-(greater than 31) (Lee et al., 2006). This empirical relationship cannot be used for data with low SSS in these regions with higher discharge due to major rivers. In the tropical Atlantic, Takahashi et al. (2014a) determined and used only one empirical relationship of TA regression for the whole tropical Atlantic basin; this relationship is similar to the one determined by Lefèvre et al. (2010), specifically for the Amazon region. In the same year, Koffi et al. (2010) determined a different TA relationship in the eastern Gulf of Guinea, with a slope that was highly different from that determined in Lefèvre et al. (2010) and Takahashi et al. (2014a). Due to the spatiotemporal variability, in the western region, an empirical relationship of C<sub>T</sub> was obtained by Bonou et al. (2016a) using SSS and time variation (year), while in the eastern region, Koffi et al. (2010) determined an empirical relationship of C<sub>T</sub> using SST and SSS (**Table 1**). It is desirable to continue studying the performance of linear regression, multiple regression or other methods to obtain a better estimation of the carbon parameters. The compilation of many data cruises, within the context of acquiring new observation



1  
2  
3  
4  
5  
6  
7  
8  
9  
10  
11  
12  
13  
14  
15  
16  
17  
18  
19  
20  
21  
22  
23  
24  
25  
26  
27  
28  
29  
30  
31  
32  
33  
34  
35  
36  
37  
38  
39  
40  
41  
42  
43  
44  
45  
46  
47  
48  
49  
50  
51  
52  
53  
54  
55  
56  
57  
58  
59  
60  
61  
62  
63  
64  
65

data, is a good means to determine existing relationships in order to have robust equations that are adaptable to the regions, leading to smaller uncertainties.

### Table 1

Data from different sources are compiled from different oceanographic data cruises (1983-2014) to compare the TA and  $C_T$  variations in the western and eastern tropical Atlantic, mainly in coastal areas adjacent to rivers. The compilation of several data cruises was used to test the reliability of the existing relationships and to reproduce the TA/ $C_T$  distribution in these transition regions. A comparative study was ~~done~~performed to emphasize the limits and differences in the variation ~~of~~in TA/ $C_T$  at the tropical Atlantic borders.

## 2. Material and Methods

### 2.1. Database and methodology

All available cruise data were extracted from oceanographic and voluntary merchant ships (20°S-20°N, 70°W-15°E) in the tropical Atlantic ~~that, which~~ is the study area where in situ data TA,  $C_T$ , SST and SSS were sampled and measured (**Figure 1**). In Figure 1, the data are shown in red and green for SSS<35 (points in black ~~color~~ indicate SSS>35). The dataset was acquired from 1983 to 2014 through 55 campaigns (**Table 2**) completed with those used in Bonou et al. ~~Al~~(2016). Conductivity, temperature and depth data acquired with CTD and bottle samples during those surveys were obtained from the Carbon Dioxide Information and Analysis Center ([http://cdiac.ornl.gov/oceans/bottle\\_discrete.html](http://cdiac.ornl.gov/oceans/bottle_discrete.html)).

### Figure 1 (Single Column)

1  
2  
3  
4  
5  
6  
7  
8  
9  
10  
11  
12  
13  
14  
15  
16  
17  
18  
19  
20  
21  
22  
23  
24  
25  
26  
27  
28  
29  
30  
31  
32  
33  
34  
35  
36  
37  
38  
39  
40  
41  
42  
43  
44  
45  
46  
47  
48  
49  
50  
51  
52  
53  
54  
55  
56  
57  
58  
59  
60  
61  
62  
63  
64  
65

**Table 2**

The TA and C<sub>T</sub> data used in this study were obtained from data cruises, and were determined by potentiometric titration from either a full curve (“Full”) or a single-point (“1-point”) titration.

The SSS database was obtained from an updated version of SSS data from 2013 by Reverdin et al. (2007). These data were used as indicators for determination of the area affected by freshwater due to rivers in the tropical Atlantic. The monthly SST data were extracted from the Objectively Analyzed air-sea Fluxes Project (OAFlux) database (with 1° of longitude and 1° of latitude). The SST data used in this study were acquired from 1958-2014, and the data are available on the Woods Hole Oceanographic Institution (WHOI) website at [oaflex.whoi.edu](http://oaflex.whoi.edu). The OAFlux project provides a synthesized product generated from the reanalysis datasets NCEP1, NCEP2, ERA40 and ERA (Yu and Weller, 2007, Yu et al., 2008).

The TA and C<sub>T</sub> relationships used were determined by different authors (see **Table 1**) to verify their limits to reproduce data compared to the observation data, especially at the eastern and western borders.

**2.2. Statistical analysis**

Statistical analysis and the ~~Mann-Whitney~~ Mann-Whitney test were used to compare two sets of data (TA, C<sub>T</sub>, SST, and SSS) from different areas (western tropical Atlantic and eastern tropical Atlantic) to determine the difference between the carbon parameters (TA and C<sub>T</sub>) in the different localities. Linear regression methods were applied to determine and test the connections between the physical parameters and carbon parameters; this method was also used to observe the best fit

1  
2  
3  
4  
5  
6  
7  
8  
9  
10 that matched the observation data. To compare these different relationships, the root mean square  
11 error (rmse) was calculated as follows:  
12  
13

$$14 \text{ rmse} = \left[ \frac{1}{n-1} \times \sum_{i=1}^n (X_i - Y_i)^2 \right]^{1/2} \quad (3);$$

15  
16  
17  
18 where  $X_i$  is the observed value and  $Y_i$  is the modeled value at time/place  $i$ .

19  
20 The ~~Kruskal-Wallis~~ test was used to identify significant differences ( $\alpha=0.05$ )  
21 between all regions. Additionally, Dunn's test was applied to identify significant differences  
22 between borders (NW, NE, SW, and SE, for  $\alpha=0.05$ ) and between hemispheres.  
23  
24  
25

### 26 27 **3. Results**

#### 28 29 **3.1. The distribution of SSS and SST anomalies in the tropical Atlantic**

30  
31 Standard deviations of SSS anomalies computed for the period from 1970-2013 using the database  
32 from Reverdin et al. (2007) actualized in 2013, allowed us to map the areas under distinct degrees  
33 of influence of freshwater input due to river discharge and/or precipitation (Figure 2). The regions  
34 presenting high SSS variability ( $SD > 1$ ) along the South American coast corresponded to coastal  
35 areas adjacent to the mouths of the Amazon and Orinoco rivers and areas along the  
36 African coastal border adjacent to the Congo, Niger and Volta river mouths. Lower  
37 variations in SSS anomalies were observed in the oceanic zone and along coastal areas not  
38 receiving large river discharge, as is the case for the NE-Brazilian coast and the northern coast  
39 of Africa. The São Francisco river in NE-Brazil (Figure 2) does not induce significant  
40 variation in the SSS due to the presence of numerous dams of hydroelectric plants along its  
41 course, drastically reducing its flow despite the extension of its drainage basin.  
42  
43  
44  
45  
46  
47  
48  
49  
50  
51  
52

53 **Figure 2 (Single Column)**

1  
2  
3  
4  
5  
6  
7  
8  
9  
10  
11  
12  
13  
14  
15  
16  
17  
18  
19  
20  
21  
22  
23  
24  
25  
26  
27  
28  
29  
30  
31  
32  
33  
34  
35  
36  
37  
38  
39  
40  
41  
42  
43  
44  
45  
46  
47  
48  
49  
50  
51  
52  
53  
54  
55  
56  
57  
58  
59  
60  
61  
62  
63  
64  
65

The SST distribution in the study area presents a seasonal zonal pattern with less variable values along the western Atlantic relative to that of the eastern Atlantic. SST along the South American coast varies from 26 to 28 °C in January and between 25 and 29 °C in July. Along the African coast, SST is higher (>27 °C) in the eastern Atlantic (0° to 5°N) in January, and lower (<26 °C) in coastal areas between the equator and 10°S in July (Figure 3).

Formatted: Font: Not Bold

**Figure 3 (Single Column)**

The annual amplitude of the SST in the western Atlantic (including 20°S-20°N; 70°W-30°W) was 3.0 °C. However, in the eastern Atlantic (including 20°S-20°N; 20°W-15°E), the amplitude of the SST was 5.7 °C (Figure 3,4).

**Figure 4 (1.5 Column)**

A subset division of the tropical Atlantic Ocean into four regions (NW, SW, NE and SE) is included according to the variability in the SST climatological. This division sought to differentiate the variations between the hemispheres and the continental borders (Figure 4).

The Kruskal-Wallis test showed significant differences ( $\alpha=0.05$ ;  $p=0.0007$ ) between all regions. Additionally, Dunn's test showed significant differences between borders (NW  $\neq$  NE;  $\alpha=0.05$ ;  $p=0.012$  and SW  $\neq$  SE;  $\alpha=0.05$ ;  $p=0.008$ ) and between hemispheres (NW  $\neq$  SW;  $\alpha=0.05$ ;  $p=0.009$  and NE  $\neq$  SE;  $\alpha=0.05$ ;  $p=0.003$ ).

1  
2  
3  
4  
5  
6  
7  
8  
9  
10  
11 For SSS<35 (freshwater influence), the statistical test also confirmed a significant difference  
12  
13 between the SST values of the eastern and western regions (~~Mann-Whitney~~Mann-Whitney test,  
14  
15  $p=0.0001$ ;  $\alpha = 0.05$ ).

### 16 17 18 **3.2. TA and C<sub>T</sub> in the tropical Atlantic**

19  
20 Three hundred ninety-two in situ coastal data samples of TA, C<sub>T</sub>, SSS and SST from the western  
21  
22 region, represented in red, were used in this study and compared to 103 data samples of TA, C<sub>T</sub>,  
23  
24 SSS and SST from the eastern region, represented in green (**Figure 1**). All these data were obtained  
25  
26 under the criterion of SSS being less than 35 psu. A significant difference was observed when the  
27  
28 selected TA and C<sub>T</sub> data (in red points) from the western Atlantic were compared with TA and C<sub>T</sub>  
29  
30 data (green points) from the eastern tropical Atlantic. At the western edge, the average value of TA  
31  
32 ( $2099.4 \pm 286.4 \mu\text{mol kg}^{-1}$ ) was obtained; this value was lower than the value obtained from the  
33  
34 eastern tropical Atlantic ( $2198 \pm 141.9 \mu\text{mol kg}^{-1}$ ) (**Table 3**), while the standard deviation indicated  
35  
36 a higher variation in TA in the western region than that obtained in the eastern region (~~Mann-~~  
37  
38 WhitneyMann-Whitney test,  $p = 0.0008$ ,  $\alpha = 0.05$ ). For the C<sub>T</sub> variable, ( $1892.2 \pm 94.2 \mu\text{mol kg}^{-1}$ )  
39  
40 and ( $1779.6 \pm 236.4 \mu\text{mol kg}^{-1}$ ) are the mean values and the standard deviation obtained,  
41  
42 respectively, at the eastern and western borders.— The standard deviation on CT in the western  
43  
44 border iswas higher than that of the eastern border, it is showing that higher variation ofin TA and  
45  
46 CT thein South America than in the African border (~~Mann-Whitney~~Mann-Whitney test,  $p =$   
47  
48  $0.00002$ ,  $\alpha = 0.05$ ).

### 49 50 **Table 3**

1  
2  
3  
4  
5  
6  
7  
8  
9  
10  
11 This result supports the higher average values of TA and  $C_T$  (**Table 3**) in the eastern region Koffi  
12 et al. (2010) and the higher TA and CT values in the Gulf of Guinea, especially in this upwelling  
13 region (**Figure 4**).  
14  
15  
16  
17

### 18 **3.3. Relevance and limitation of existing relations for TA and $C_T$ in the tropical Atlantic.**

19  
20 The relationships proposed by Lefèvre et al. (2010), Koffi et al. (2010) and Bonou et al. (2016a)  
21 (**Table 4**) were used to compute TA and  $C_T$  and to observe their spatial relevance and limitations  
22 in the tropical Atlantic. The data in red and green samples have SSS ~~is~~ values lower than 35, while  
23 the data in black correspond to ~~that~~ those of the regions where SSS is higher than 35 (**Figure 1**).  
24  
25  
26  
27

#### 28 **Table 4**

29 Observations of  $SSS < 35$  in the western border are due to the higher influence of rivers and  
30 freshwater due to the retroflexion of Amazonian waters by the North Brazilian Current (NBC) and  
31 into the NECC, which is beyond the influence of rainfall in the equatorial region due to the ITCZ  
32 (~~InterTropical Convergence Zone~~-intertropical convergence zone). In this region, the empirical  
33 relationship proposed by Lefèvre et al. (2010) represents the TA observations better than the  
34 relationships proposed by Koffi et al. (2010) (**Figure 5A**). The standard deviation of TA from  
35 Lefèvre et al. (2010) was  $28.6 \mu\text{mol.kg}^{-1}$ , while that obtained for TA by Koffi et al. (2010) was  $64.8$   
36  $\mu\text{mol.kg}^{-1}$  (**Table 4**). The greatest discrepancies occur for data with  $SSS < 30$ .  
37  
38  
39  
40  
41  
42  
43  
44  
45

#### 46 **Figure 5 (Single Column)**

47  
48  
49  
50 The opposite trend was observed in the eastern region, where the relationship described in Koffi  
51 et al. (2010) is better at reproducing the observation data than that described in Lefèvre et al.  
52  
53  
54  
55  
56  
57  
58  
59  
60  
61  
62  
63  
64  
65

1  
2  
3  
4  
5  
6  
7  
8  
9  
10  
11  
12  
13  
14  
15  
16  
17  
18  
19  
20  
21  
22  
23  
24  
25  
26  
27  
28  
29  
30  
31  
32  
33  
34  
35  
36  
37  
38  
39  
40  
41  
42  
43  
44  
45  
46  
47  
48  
49  
50  
51  
52  
53  
54  
55  
56  
57  
58  
59  
60  
61  
62  
63  
64  
65

(2010) (**Figure 6**). The rmse value of TA was  $12.5 \mu\text{mol kg}^{-1}$ , which was obtained from the relationship from Koffi et al. (2010) in the eastern region. This rmse value TA is almost two times lower than that obtained with the relationship of Lefèvre et al. (2010) (**Table 4**). This result ~~is in agreement~~ agrees with that obtained in Lefèvre et al. (2010), which showed the best fit of TA with SSS when using Koffi et al. (2010).

### Figure 6 (1.5 Column)

### 3.4. Biological processes

In the western and eastern tropical Atlantic, biological consumption is one of the processes that ~~influence~~ influences the variation ~~of~~ in the carbon parameters around ~~the~~ tropical edges (Cooley et al., 2007; da Cunha et al., 2013; Araujo et al., 2014).

As explained above, the surface  $C_T$  concentration is influenced by lateral and vertical mixing of water with different levels of  $C_T$  (the transport effect), photosynthesis and oxidation of organic matter (the biological effect) and changes in temperature and salinity (Takahashi et al., 1993; Lee et al., 2000). However, these effects are ~~direct~~ directly or indirectly correlated with SST, but the trends often differ seasonally and geographically.

According to Koffi et al. (2010), equatorial upwelling and coastal upwelling along the eastern boundary merge to form a cold tongue during the main upwelling season, and the cold tongue undergoes advection westward by the South Equatorial Current (SEC). This cold tongue transports  $\text{CO}_2$ -rich waters, and  $f\text{CO}_2$  increases as the surface water temperature increases toward the west.

The Guinea Current (GC) and ~~(SEC)~~ are influenced by several fluvial contributions, including the Volta River ( $4^\circ\text{N}$ - $0^\circ\text{S}$ ), Niger River ( $3^\circ\text{N}$ ,  $8^\circ\text{E}$ ) and Congo River ( $-6^\circ\text{S}$ ,  $12^\circ\text{E}$ ) (Koffi et al., 2010).

1  
2  
3  
4  
5  
6  
7  
8  
9  
10  
11  
12  
13  
14  
15  
16  
17  
18  
19  
20  
21  
22  
23  
24  
25  
26  
27  
28  
29  
30  
31  
32  
33  
34  
35  
36  
37  
38  
39  
40  
41  
42  
43  
44  
45  
46  
47  
48  
49  
50  
51  
52  
53  
54  
55  
56  
57  
58  
59  
60  
61  
62  
63  
64  
65

The eastern border is strongly affected by biological activity (NE and SE). The average  $C_T$  was 2056  $\mu\text{mol kg}^{-1}$ , which is close to that of the Atlantic Ocean, as indicated by Millero (2006).

The satellite data through the MODIS-Aqua sensor were used for the study region. The highest concentrations of chlorophyll-*a* are observed in the coastal regions near the Amazon River, Orinoco River, Congo River and NW Africa (coastal upwelling) (Figure 7).

## 4. Discussion

### 4.1. Analysis of the regions influenced by tropical Atlantic Rivers

The ~~distribution of the~~ standard deviation distribution of anomalies was used by Bonou et al. (2016a) to identify regions with higher variations of in the variables considered. In our work, this method was applied to investigate the ~~sub-regions~~ subregions of the tropical Atlantic characterized by higher variations in SSS (Figure 2). The fact that almost all the regions of the tropical Atlantic presenting large ~~SDSDs~~ of SSS anomalies were located near tropical rivers presenting high discharge corroborates that this method is robust to ~~identify~~ identifying the influence of its discharge on salinity.

The standard deviation of SSS was an anomaly with values between 0.2 and 2.0 for the coastal regions of the study area. There is a significant difference between the SSS anomalies (~~Mann-Whitney~~ Mann-Whitney test,  $p=0.0005$ ;  $\alpha = 0.05$ ) at the western and eastern borders of the tropical Atlantic. The hydric balance of the Amazon and Orinoco Rivers at the western edge is greater than the balance of the Congo, Niger and Volta Rivers at the eastern border (Dai and Trenberth, 2002; Cai et al., 2008; da Cunha et al., 2013; Araujo et al., 2014). According to Bonou et al. (2016a), in the tropical Atlantic, the variation in SSS is higher in the western region, with SSS values between 1 and 38.



1  
2  
3  
4  
5  
6  
7  
8  
9  
10  
11  
12  
13  
14  
15  
16  
17  
18  
19  
20  
21  
22  
23  
24  
25  
26  
27  
28  
29  
30  
31  
32  
33  
34  
35  
36  
37  
38  
39  
40  
41  
42  
43  
44  
45  
46  
47  
48  
49  
50  
51  
52  
53  
54  
55  
56  
57  
58  
59  
60  
61  
62  
63  
64  
65

The western tropical Atlantic shows a higher variability in SSS and a less pronounced seasonal variability in SST. On the other hand, the eastern tropical Atlantic presents a lower variability in SSS but a strong seasonal variability in SST (**Figures 2, 3 and 4**). This area ~~experiencing~~ coastal upwelling (Schneider et al., 1997; Dale et al., 2002) ~~were, where~~ a rise ~~of~~ cold-water masses rich in nutrients and CO<sub>2</sub> is observed and ~~where~~ surface coastal water is pushed ~~off-shore~~ offshore by Ekman divergence.

The SSS is a physical parameter that has a high correlation with carbon parameters, and its variability is believed to impact carbon parameters. In the Tropical Atlantic, the SSS is highly correlated with TA and CT (Bonou et al. (2016a), Koffi et al. (2010), Lefèvre et al. (2010); therefore, the stronger influence of the Amazon and Orinoco Rivers in the western tropical Atlantic is one explanation for the difference observed in the carbon parameters between the eastern and western regions.

#### **4.2. Pertinence of existing relations to the tropical Atlantic.**

The results presented in **Figures 5A** and **5B** show that the relationships from Lefèvre et al. (2016) are adapted in the western tropical Atlantic region mainly in the Amazon and Orinoco Rivers, while the relationship from Koffi et al. (2010) reproduces the observations in the eastern tropical Atlantic well, mainly in the Gulf of Guinea.

In the central basin of the tropical Atlantic, the results with  $SSS \geq 35$  showed that the behavior was very close between the two empirical relationships (**Figure 5C**). The relationship from Lefèvre et al. (2016) had a slightly higher rmse value than that obtained from the relationship from Koffi et al. (2010) (20.5 and 19.2  $\mu\text{mol kg}^{-1}$ , respectively). According to these results, the use of the two empirical relationships yielded similar TA values in the central region when  $SSS \geq 35$  psu.

1  
2  
3  
4  
5  
6  
7  
8  
9  
10  
11  
12  
13  
14  
15  
16  
17  
18  
19  
20  
21  
22  
23  
24  
25  
26  
27  
28  
29  
30  
31  
32  
33  
34  
35  
36  
37  
38  
39  
40  
41  
42  
43  
44  
45  
46  
47  
48  
49  
50  
51  
52  
53  
54  
55  
56  
57  
58  
59  
60  
61  
62  
63  
64  
65

Almost all TA data with  $SSS \geq 37$  are clustered around the green line, which is the line represented by the relationships from Koffi et al. (2010). Data with  $SSS \geq 37$  are located in the [SEC region of the SEC](#) (Figure 6), which ~~is extended~~ extends to the western part. This result means that the relationship from Koffi et al. (2010), as determined in the eastern region, can be extended into the western part of the SEC.

Analysis of the [proposed relationships](#) ~~proposed~~ used to determine  $C_T$  is more complicated, at least regarding its graphical representation. In the eastern region, Koffi et al. (2010) determined  $C_T$  relationships using SSS and SST, while Bonou et al. (2016a) determined a  $C_T$  relationship using only the SSS function but still considered its temporal variation (Table 3) in the western tropical Atlantic region. The  $C_T$  relationships in both regions (western and eastern) do not depend only on SSS and TA relationships. In this case,  $C_T$  cannot be estimated only as a function of a single SSS parameter, and the statistical results are presented in Table 4 (Bonou et al., 2016b).

In the western tropical Atlantic, the rmse value was obtained from the estimated  $C_T$  derived from Bonou et al. (2016a), and this value was  $41.1 \mu\text{mol kg}^{-1}$  considering that the relationship from Koffi et al. (2010) gives  $47.9 \mu\text{mol kg}^{-1}$  as the rmse value. In the eastern region, the rmse value obtained from the estimated  $C_T$  relationship from Koffi et al. (2010) was  $28.11 \mu\text{mol kg}^{-1}$ , while from Bonou et al. (2016a), the rmse value was  $29.6 \mu\text{mol kg}^{-1}$ . In the oceanic region ( $SSS \geq 35$ ), the rmse values were also similar between the two empirical relationships ( $34.7$  and  $35.1 \mu\text{mol kg}^{-1}$  for Koffi et al. (2010) and Bonou et al. (2016a), respectively). In fact, the greatest variation in SST observed in the eastern edge of the basin contributes to the  $C_T$  equation since SST is one of the key state variables that influence the carbon cycle in this region (Lefèvre et al., 2008; Koffi et al., 2010, Bonou et al., 2016b). On the other hand, the empirical relationships of  $C_T$  proposed for the western edge do not ~~take into account~~ consider SST because their variation is lower at the western edge than

1  
2  
3  
4  
5  
6  
7  
8  
9  
10  
11  
12  
13  
14  
15  
16  
17  
18  
19  
20  
21  
22  
23  
24  
25  
26  
27  
28  
29  
30  
31  
32  
33  
34  
35  
36  
37  
38  
39  
40  
41  
42  
43  
44  
45  
46  
47  
48  
49  
50  
51  
52  
53  
54  
55  
56  
57  
58  
59  
60  
61  
62  
63  
64  
65

in the eastern region (Lefèvre et al., 2010; Ibánhez et al., 2015; Bonou et al., 2016a). According to Key et al. (2004), the surface  $C_T$  distribution is affected by physical processes; however, the pattern is more similar to that of nutrients (e.g., nitrate) than to that of salinity. This is because  $C_T$  concentrations are more strongly affected by biology than ~~those of TA/TA concentrations~~.

### 4.3. Lithological composition of basins and influence of plumes

The different rock types that dominate the river basins influence the input of  $CO_2$  through rock weathering and through riverine transport of inorganic carbon to the ocean. The chemical erosion of inorganic materials consists of dissolving or hydrolyzing primary minerals of rocks and soils. The chemical reactions require  $CO_2$  and release  $C_T$  (mainly as  $HCO_3^-$ ). Thus, different rock types have different  $CO_2$  consumption rates. According to Amiotte-Suchet et al. (2003), high  $CO_2$  consumption rates are observed in carbonate rocks, moderate  $CO_2$  consumption rates are observed in basalts plus shales, and low  $CO_2$  consumption rates are observed in shales plus and sands/sandstones. Thus, the Amazon and Orinoco Rivers have high  $CO_2$  consumption rates, and the Congo and Niger Rivers have moderate and low  $CO_2$  consumption rates. Araujo et al. (2014) observed that the contribution of the mean  $CO_2$  fluxes consumed by the total  $HCO_3^-$  ~~rivers/river~~ flux was 82 and 88% for the western border and eastern border, respectively. These authors also indicated that during a dry period, the atmospheric  $CO_2$  flux consumed through rock weathering was lower than that during a more humid period. However, middle-latitude and subtropical larger rivers have high bicarbonate ( $HCO_3^-$ ) concentrations and fluxes because of the abundant distribution of carbonate minerals in their drainage basins. In contrast, tropical larger rivers ~~have low  $HCO_3^-$  concentrations~~, such as the Amazon and Orinoco Rivers, ~~have low  $HCO_3^-$  concentrations~~ (Cai et al., 2010).

Formatted: Subscript  
Formatted: Superscript

1  
2  
3  
4  
5  
6  
7  
8  
9  
10  
11  
12  
13  
14  
15  
16  
17  
18  
19  
20  
21  
22  
23  
24  
25  
26  
27  
28  
29  
30  
31  
32  
33  
34  
35  
36  
37  
38  
39  
40  
41  
42  
43  
44  
45  
46  
47  
48  
49  
50  
51  
52  
53  
54  
55  
56  
57  
58  
59  
60  
61  
62  
63  
64  
65

Large rivers also generate offshore plumes that are characterized by high buoyancy and biological productivity because of their low salinities, high levels of nutrients, and suspended and dissolved terrestrial materials (Higgins et al., 2006; Kouamé et al., 2009; Kang et al., 2013). As a result, the chemical, geological, biological and physical environments of the adjacent marginal seas are affected. Low-salinity regions at the eastern edge (SSS <35) in the Atlantic Ocean can be found in two regions according to Bakker et al. (1999): one north of the equator and one near the Congo River. Van Bennekom et al. (1978) and Vangriesheim et al. (2009) showed that the influence of the Congo River ranges from -3.5° to -6.5° latitude and reaches 6.5° E in the Atlantic Ocean (700 km offshore).

In the Atlantic Ocean, the dispersal of the Amazon River water leads to a brackish water plume that can exceed 10<sup>6</sup> km<sup>2</sup>, reaching latitudes as far from the river mouth as 30°W (Coles et al., 2013) or even 25°W when the North Equatorial Countercurrent (NECC) is strong (Lefèvre et al., 1998). Recently, Ibánhez et al. (2017) compared the monthly precipitation rate with the monthly SSS in five regions of the tropical Atlantic. They found highly significant linear relationships of precipitation with SSS across the western Atlantic basin. The extension of the Amazon River plume was highly significant, ranging from 0.25 to 1.60 × 10<sup>6</sup> km<sup>2</sup>, after removing the influence of rainfall. In Tropical Atlantic regions, low salinity patches are related to large rivers, such as the Amazon (5413 km<sup>3</sup> year<sup>-1</sup>), followed by the Congo (1263 km<sup>3</sup> year<sup>-1</sup>) and Orinoco (1170 km<sup>3</sup> year<sup>-1</sup>), spreading freshwater by surface oceanic circulation (Araujo et al. 2014).

According to (Araujo et al. (2014), significant differences were observed between the large estuarine systems of the Atlantic Ocean. The authors indicated that C<sub>T</sub> and TA showed significant differences between the eastern (Volta, Niger and Congo Rivers) and western (Orinoco, Amazon, São Francisco and Paraíba do Sul ~~rivers~~Rivers) estuaries. Other important parameters also showed significant differences, such as pCO<sub>2</sub> and dissolved organic carbon (DOC). According to these

1  
2  
3  
4  
5  
6  
7  
8  
9  
10  
11  
12  
13  
14  
15  
16  
17  
18  
19  
20  
21  
22  
23  
24  
25  
26  
27  
28  
29  
30  
31  
32  
33  
34  
35  
36  
37  
38  
39  
40  
41  
42  
43  
44  
45  
46  
47  
48  
49  
50  
51  
52  
53  
54  
55  
56  
57  
58  
59  
60  
61  
62  
63  
64  
65

authors, DOC is higher in the eastern region; this would affect coastal concentrations in that region, increasing  $C_T$  levels in the adjacent coastal region. Additionally, TA is mainly affected by the chemical reactions of the different types of rocks in the soils of the hydrographic basins, which are carried to the coastal region via runoff

~~Basing~~Based on the approaches of Ternon et al. (2000), Körtzinger (2003), Cooley and Yager (2006) and Araujo et al. (2014), ~~a~~ simple conservative mixing model ~~has been~~ was used to calculate the proportions of  $C_T$  in western rivers (Amazon and Orinoco) and eastern rivers (Niger, Volta and Congo) for ~~the~~ plume water and seawater in a given plume sample (Figure 10). This ~~approach of~~ mixing model approach has been widely detailed in the supplementary material of Araujo et al. (2014). ~~It is~~ assumed that the effects of precipitation and evaporation on the carbon and freshwater mass balances are small compared to the river (Cooley and Yager, 2006) over the first 10 m-deep plume. Additional variations in  $CT$  not attributable to mixing were then ascribed to biology ( $CT_{bio}$ ). Using the mixing equations of Araujo et al. (2014), we used TA, SSS and  $CT$  to estimate the excess or deficit of  $CT_{bio}$  in the east and west coastal regions ( $TA_{bio}$  calculation is not necessary here, as TA is considered ~~as a~~ conservative parameter). ~~Positive~~ values of  $\Delta CT_{bio}$  indicate an inorganic carbon deficit, implying that the respiration process exceeds the respiration process. Thus, the system is considered to be autotrophic, while negative  $CT$  values indicate excess  $CT$ , suggesting that respiration > production, and the system is considered heterotrophic. The results showed that ~~both~~ regions have had negative  $CT_{bio}$  values in the estuarine region, indicative of excess  $CT$ . Outside the plume, the values oscillate between positive and negative; however, the mean values of the gradients indicate excess  $CT$ . In the western region, 7% of the  $CT$  excess (bio) average across the entire saline gradient ~~has been~~ was obtained, while in the eastern region, this percentage was lower (0.2%). According to these results, ~~it considered that~~ the primary productivity in the eastern region is higher ~~when compared to that of~~ than that in the western region

1  
2  
3  
4  
5  
6  
7  
8  
9  
10  
11  
12  
13  
14  
15  
16  
17  
18  
19  
20  
21  
22  
23  
24  
25  
26  
27  
28  
29  
30  
31  
32  
33  
34  
35  
36  
37  
38  
39  
40  
41  
42  
43  
44  
45  
46  
47  
48  
49  
50  
51  
52  
53  
54  
55  
56  
57  
58  
59  
60  
61  
62  
63  
64  
65

(~~Figure 10~~ [Figure 10](#) a and b). Additionally, we have to consider that the extension of the plumes differs, and the saline values are smaller in the western region, generating a greater amplitude of variation between the CT values. The concentrations of  $\text{HCO}_3^-$  (the main component of CT coming from the rocks) in the eastern region are higher; however, the freshwater flow is greater in the western region. The observed concentrations showed that the western region has an average CTbio excess of ~~92  $\mu\text{mol}$~~  [92  \$\mu\text{mol}\$](#)   $\text{kg}^{-1}$ , while the eastern region has an [average CTbio](#) excess of ~~3  $\mu\text{mol}$~~  [3  \$\mu\text{mol}\$](#)   $\text{kg}^{-1}$ . In estuarine zones, these excesses of CT are greater. In the western region, ~~can reach~~ [it reached](#) 14%, while in the estuarine zone of the eastern region, it was 1%.

#### 4.4. Regional differences in carbonate chemistry

The ratio of TA to the dissolved inorganic carbon concentration (TA: $C_T$ ) is of particular interest because it serves as an indicator of the relative abundance of carbonate species (e.g.,  $\text{HCO}_3^-$  and  $\text{CO}_3^{2-}$ ) in seawater. According to Wang et al. (2013), for a specific temperature and pressure, the  $\text{CO}_2$  system parameters, such as the aragonite saturation state and pH value, are closely correlated with this ratio, which has been widely used in studies of seawater carbonate chemistry (Zeebe and Wolf-Gladrow, 2001).

Differences in the seawater TA:  $C_T$  imply, for example, differences in buffer intensity, also called buffer capacity (Revelle factor). The buffer intensity of the seawater carbonate system is at a minimum when  $\text{CO}_3^{2-} \sim \text{CO}_{2\text{aq}}$ , where the TA and  $C_T$  concentrations are approximately equal (i.e., when TA:  $C_T \approx 1$ ).

In [Figure 8](#) (corresponding to the NW region), water with a relatively low salinity (<35) dominates. A linear regression line derived from the SSS=20-37 portion of the TA-SSS plot produced a very low TA. In contrast, in [Figure 8C](#) (SW region), high [SSS](#) values ~~of SSS~~ (>32) are observed in

1  
2  
3  
4  
5  
6  
7  
8  
9  
10  
11  
12  
13  
14  
15  
16  
17  
18  
19  
20  
21  
22  
23  
24  
25  
26  
27  
28  
29  
30  
31  
32  
33  
34  
35  
36  
37  
38  
39  
40  
41  
42  
43  
44  
45  
46  
47  
48  
49  
50  
51  
52  
53  
54  
55  
56  
57  
58  
59  
60  
61  
62  
63  
64  
65

the TA-SSS plot. This region is not affected by major river discharge. The variations in TA and SSS are assigned to physical factors, especially the balance between precipitation and evaporation. The eastern edge (**Figure 8B** and **Figure 8D**) has regions with high productivity associated with the discharge of large rivers, such as the Niger and Congo Rivers. In **Figure 8B**, a very low TA was observed at zero salinity. As indicated in [Section section-3.5](#), low rates of CO<sub>2</sub> consumption have been reported for the Niger and Congo Rivers. As a result, the chemical, geological, biological and physical environments of coastal areas are affected. Low-salinity regions at the eastern edge (SSS <35) in the Atlantic Ocean can be found in two regions according to Bakker et al. (1999): one north of the equator and one near the Congo River. In contrast, in high-salinity offshore waters (>32), TA and SSS exhibited a tight linear correlation with an elevated TA.

The in-situ ~~observation the~~observations of TA and C<sub>T</sub> obtained ~~at~~in the coastal ~~region~~regions of Africa and Brazil show significant differences (Bonou et al., 2016b). The biogeochemical composition of each border is different, and many different processes occur at each border, which are different from one another, including in the SSS≥35 regions.

### Figure 8

The values observed here showed typical values for tropical waters, with a slight increase in the average values in the TA:-CT (SW region; **Figure 9C**).

~~The figure Figure 9B to figure Figure 9D shows to be~~show a relatively well-buffered TA: C<sub>T</sub> > 1.15, while ~~figure Figure 9A, indicate indicates~~ a minor buffering capacity (TA:C<sub>T</sub>=1.1). A lower buffer capacity may respond to coastal acidification, such as ~~may accompany~~ increases in atmospheric CO<sub>2</sub> or eutrophication events.

1  
2  
3  
4  
5  
6  
7  
8  
9  
10  
11  
12  
13  
14  
15  
16  
17  
18  
19  
20  
21  
22  
23  
24  
25  
26  
27  
28  
29  
30  
31  
32  
33  
34  
35  
36  
37  
38  
39  
40  
41  
42  
43  
44  
45  
46  
47  
48  
49  
50  
51  
52  
53  
54  
55  
56  
57  
58  
59  
60  
61  
62  
63  
64  
65

Biogeochemical processes such as photosynthesis, respiration (P-R), and air-sea CO<sub>2</sub> exchange also change the C<sub>T</sub>. Changes in the C<sub>T</sub> in regions with high fluvial discharge can alter these processes; and consequently ~~reduce~~ ~~ing~~ ~~reduce~~ the TA:-C<sub>T</sub> ratio. In the SW region, TA:-CT is high, making conditions more favorable for oceanic uptake of atmospheric CO<sub>2</sub>.

**Figure 9**

**5. Conclusions**

The tropical Atlantic Ocean receives an important amount of carbon from the African and South American continents, which present different features at their oceanic borders. In this work, the comparative study of TA and C<sub>T</sub> data from the coastal region of Africa and Brazil shows significant differences between these variables (~~Mann-Whitney~~ ~~Mann-Whitney~~ test,  $\alpha=0.05$ ,  $p=0.0001$ ). These differences are explained by the differences ~~of~~ ~~in~~ biological activities, the influence of rivers, and the composition of biogeochemicals in different coastal areas. At the western tropical border, the minimum values of the carbon parameters were obtained, while higher values of the carbon parameters were obtained in the eastern tropical Atlantic border. The biogeochemical composition of each border is different, and many different processes occur at each border. The coastal upwelling process at the eastern border contributes to the higher CO<sub>2</sub> concentrations obtained in the eastern coastal area compared to those obtained at the western edge. This physical process increases the CO<sub>2</sub> parameters in surface water, followed by an additional physical process that transports the rich water masses from the African coast to the Brazilian coast through oceanic circulation (SEC). The river characteristics at each border are different in terms of their physical and biological activities and chemical composition. The existing TA and C<sub>T</sub> relationships present spatial limitations, and the use of the empirical TA relationship determined by Lefèvre et al. (2010)



1  
2  
3  
4  
5  
6  
7  
8  
9  
10  
11  
12  
13  
14  
15  
16  
17  
18  
19  
20  
21  
22  
23  
24  
25  
26  
27  
28  
29  
30  
31  
32  
33  
34  
35  
36  
37  
38  
39  
40  
41  
42  
43  
44  
45  
46  
47  
48  
49  
50  
51  
52  
53  
54  
55  
56  
57  
58  
59  
60  
61  
62  
63  
64  
65

~~to~~for the observation data at the eastern border presents high root mean square error values. The similarity between the relationships from Takahashi et al. (2014) and Lefèvre et al. (2010) suggests that calculation of the carbon parameters in the eastern region, using one of these relationships, will lead to a higher root mean square error value. Otherwise, the climatological map determined by Takahashi et al. (2014) in the eastern region using this ~~relation~~relationship may be affected by an important bias compared to that in other regions. On the other hand, the TA relationship determined by Koffi et al. (2010) is not a better relationship to be applied to the coastal data in the Amazon plume. However, we found that their relationship with TA can be extended to the southwestern part, mainly in the SEC region, for data with  $SSS \geq 37$ .

In coastal regions, the biogeochemical composition of each border is different, and many different processes occur at each border, principally regions that include values for  $SSS < 35$ .

#### ~~Authors~~Author contributions

All authors contributed extensively to the interpretation of the results and to ~~the~~ writing of the manuscript.

#### Acknowledgments

We are grateful to the SNAPO-CO<sub>2</sub> (Service National d'Analyses des Paramètres du CO<sub>2</sub>) at LOCEAN (Paris) for the TA and C<sub>T</sub> analyses from Plumand, Amandes, PIRATA, Colibri, Aramis, Rio Blanco, Camadas Finas and Bioamazon cruises). We acknowledge the scientific and crew members of the NOc. Antares and NO Antea for their help at sea and to the Marine Nantaise and Hamburg Sud for allowing sampling onboard their merchant ships. We thank IRD for the financial support and the financial contributions from INCT AmbTropic, CNPq/FAPESB (Grants 565054/2010-4 and 8936/2011), LEFE CYBER program, AIRD-FAPEMA BIOAMAZON

1  
2  
3  
4  
5  
6  
7  
8  
9  
10  
11  
12  
13  
14  
15  
16  
17  
18  
19  
20  
21  
22  
23  
24  
25  
26  
27  
28  
29  
30  
31  
32  
33  
34  
35  
36  
37  
38  
39  
40  
41  
42  
43  
44  
45  
46  
47  
48  
49  
50  
51  
52  
53  
54  
55  
56  
57  
58  
59  
60  
61  
62  
63  
64  
65

project, and the EU integrated project CARBOCHANGE (Grant 264879). F. Bonou acknowledges Yves du Penhoat, Alexis Chaigneau and IRD, and JEAI for their technical support. C. Noriega acknowledges the National Council for Scientific and Technological Development – CNPq (Project 465634/2014-1; process number 370821/2019-0; INCT program). This work is a contribution of the Brazilian Research Network on Global Climate Change, Rede CLIMA (<http://redeclima.ccst.inpe.br/>).

**Conflict of Interest Statement:** The authors declare that the research was conducted in the absence of any commercial or financial relationships that could be construed as a potential conflict of interest.

1  
2  
3  
4  
5  
6  
7  
8  
9  
10  
11 **List of figures**  
12  
13

14 **Figure 1.** Routes of the different cruises (55 cruises), indicating the geographical positions of the  
15 total alkalinity (TA) samples in the Tropical Atlantic. The red and green colors represent samples  
16 collected from the western and eastern tropical Atlantic, respectively, with  $SSS < 35$ , and the black  
17 points are data with  $SSS \geq 35$  in the tropical Atlantic.  
18  
19

20  
21 **Figure 2.** Standard deviation of SSS anomalies for the period from 1970-2013, showing the  
22 coastal regions with greater variability in SSS under the influence of rivers.  
23  
24

25 **Figure 3.** Monthly distribution of SST ( $^{\circ}\text{C}$ ) for January and July during the period of 1958-2014  
26 in the tropical Atlantic.  
27  
28

29 **Figure 4.** SST climatology of the western and eastern regions for the 1958-2014 period (OAFlux  
30 database - <http://oaflux.whoi.edu/>). NW ( $-70^{\circ}\text{W}$  to  $-35^{\circ}\text{W}$ ;  $0^{\circ}$  to  $20^{\circ}\text{N}$ ); NE ( $-35^{\circ}\text{W}$  to  
31  $+10^{\circ}\text{W}$ ;  $0^{\circ}$  to  $20^{\circ}\text{N}$ ); SW ( $-50^{\circ}\text{W}$  to  $-15^{\circ}\text{W}$ ;  $0^{\circ}$  to  $-20^{\circ}\text{S}$ ); SE ( $-15^{\circ}\text{W}$  to  $+10^{\circ}\text{W}$ ;  $0^{\circ}$  to -  
32  $20^{\circ}\text{S}$ ).  
33  
34  
35

36 **Figure 5.** Comparisons among: **A)** empirical relationships of Koffi et al. (2010) and Lefèvre et al.  
37 (2010) for the estimated TA applied to data with  $SSS < 35$  in the western tropical Atlantic; **B)**  
38 empirical relationships of Koffi et al. (2010) and Lefèvre et al. (2010) for the estimated TA  
39 applied to data with  $SSS < 35$  in the eastern tropical Atlantic; **C)** empirical relationships of Koffi  
40 et al. (2010) and Lefèvre et al. (2010) for the estimated TA applied to data with  $SSS \geq 35$  in the  
41 central tropical Atlantic.  
42  
43  
44

45 **Figure 6.** Localization of data with  $SSS \geq 37$  around Koffi et al. (2010) lines in green and of data  
46 with  $SSS \geq 35$  in black in the central region of the tropical Atlantic.  
47  
48  
49

50 **Figure 7.** Annual average data from 10 years (2006-2015) of the chlorophyll-*a* concentrations in  
51 the tropical Atlantic Ocean (MODIS-Aqua; 4 km resolution), obtained from:  
52 <https://giovanni.gsfc.nasa.gov/giovanni/>. (Data access: 2017.05.09).  
53  
54

1  
2  
3  
4  
5  
6  
7  
8  
9  
10  
11  
12  
13  
14  
15  
16  
17  
18  
19  
20  
21  
22  
23  
24  
25  
26  
27  
28  
29  
30  
31  
32  
33  
34  
35  
36  
37  
38  
39  
40  
41  
42  
43  
44  
45  
46  
47  
48  
49  
50  
51  
52  
53  
54  
55  
56  
57  
58  
59  
60  
61  
62  
63  
64  
65

**Figure 8:** TA-SSS relationship in the different sub-region-subregions in the Atlantic Ocean.

**Figure 9:** TA:C<sub>T</sub> for the NW region (A); NE region (B); SW region (C) and SE region (D). The black line TA:C<sub>T</sub> =1; the dashed line ~~indicate~~ indicates the tendency of the observed values. 4.7. C<sub>T</sub> and TA normalization in the tropical Atlantic.

**Figure 10:** C<sub>T</sub> bio (C<sub>Texcess</sub>) derived from the mixing model in function SSS (a) in the western region and (b) in the eastern region

### Tables

**Table 1.** Empirical carbon relationships available for the regions near tropical Atlantic Rivers.

REGION	EMPIRICAL RELATION	REFERENCE
Western	TA = 58 * SSS+265	Lefèvre et al. (2010)
	C <sub>T</sub> = 50.1*SSS+0.9*(Year-1989) +198	Bonou et al. (2016a)
Eastern	TA = 65.52*SSS+2.50	Koffi et al. (2010)
	C <sub>T</sub> = 51.71*SSS-12.79*SST +507.82	Koffi et al. (2010)
Tropical Atlantic	TA = 58.25*SSS+270.9	Takahashi et al. (2014a)

1  
2  
3  
4  
5  
6  
7  
8  
9  
10  
11  
12  
13  
14  
15  
16  
17  
18  
19  
20  
21  
22  
23  
24  
25  
26  
27  
28  
29  
30  
31  
32  
33  
34  
35  
36  
37  
38  
39  
40  
41  
42  
43  
44  
45  
46  
47  
48  
49  
50  
51  
52  
53  
54  
55  
56  
57  
58  
59  
60  
61  
62  
63  
64  
65

**Table 2.** Additional data cruises used in this paper with measurements of TA and C<sub>T</sub> compiled with data from Bonou et al. (2016) for all tropical Atlantic Ocean data.

CRUISE	PERIOD	SHIP	REFERENCE	METHODOLOGY		PRECISION/ ACCURACY	
				TA <sup>a</sup>	C <sub>T</sub>	TA (μmol kg <sup>-1</sup> )	C <sub>T</sub> (μmol kg <sup>-1</sup> )
TTOTASSV	Dec 1982- Jan 1983	<i>R/V Knorr</i>	Takahashi et al.(2014b)	-	-	-	-
AJAX_1983	Oct 1983- Fev 1984	<i>R/V Knorr</i>	Chipman et al. (2007)	-	-	-	-
SAVE-1	Nov-1987	<i>R/V Knorr</i>	Takahashi et al. (1995)	-	-	-	-
SAVE-2	Dec-1987	<i>R/V Knorr</i>	Takahashi et al. (1995)	-	-	-	-
SAVE-3	Jan-1988	<i>R/V Knorr</i>	Takahashi et al. (1995)	-	-	-	-
WOCE-A16C (SAVE)	Mar-Apr 1989	<i>R/V Melville</i>	Takahashi et al. (1989)	-	-	±2/±2	±2/±2
CITHER 1	Jan- Mar 1993	<i>R/V Atalante</i>	Oudot et al. (1995)	-	Chromatography	-	-
EGEE-1	Jun-Jul 2005	<i>R/V Antea</i>	Koffi et al. (2010)	Full	-	±2/±2	±2/±2
EGEE-2	Sep 2005	<i>R/V Antea</i>	Koffi et al. (2010)	Full	-	-	-
EGEE-3	Mai-Sep 2006	<i>R/V Antea</i>	Koffi et al. (2010)	Full	-	-	-
EGEE-5	Jun-Jul 2007	<i>R/V Antea</i>	Koffi et al. (2010)	Full	-	-	-
EGEE-5	Jun-Jul 2007	<i>R/V Antea</i>	Koffi et al. (2010)	Full	-	-	-
EGEE-6	Set 2007	<i>R/V Antea</i>	Koffi et al. (2010)	Full	-	-	-
CITHER 2-1	Jan-Mar 1994	<i>R/V Maurice Ewing</i>	Rios et al. (2005)	-	SOMMA	±1.2/±1.2	±1.64/±1.6
WOCE-A15	Abr-May 1994	<i>R/V Knorr</i>	Goyet et al. (1995)	Full	Colorimetry	-	-
METEOR 68/3	Jul-Aug 2006	<i>R/V Meteor</i>	Körtzinger & Steinhoff (2012)	Full	SOMMA	-	-
AMT7	Set-Oct 1998	<i>RRS James Clark Ross</i>	Lefèvre et al. (2002)	-	SOMMA	-	-
METEOR 80/1	Oct-Nov 2009	<i>R/V Meteor</i>	Körtzinger et al. (2012)	Full	SOMMA	-	-
FICARAM_X V	Mar-May 2013	<i>Hisperides</i>	Perez et al. (2013)	Full	-	-	-
CARINA.ATL	1999-2004	<i>Various ships</i>	This Study	Full	Potentiometry	-	-

<sup>a</sup>Determined by potentiometric titration, either a full curve (“Full”) or a single-point (“1-point”) titration. No TA was measured during the AMT7 cruise.

14  
15  
16  
17  
18  
19  
20  
21  
22  
23  
24  
25  
26  
27  
28  
29  
30  
31  
32  
33  
34  
35  
36  
37  
38  
39  
40  
41  
42  
43  
44  
45  
46  
47  
48  
49  
50  
51  
52  
53  
54  
55  
56  
57  
58  
59  
60  
61  
62  
63  
64  
65

**Table 3.** Descriptive statistics (minimum as min, maximum as max, mean and standard deviation as STD) of TA and C<sub>T</sub> in the eastern region (103 data points) and western region (392 data points).

REGION	TA (μmol kg <sup>-1</sup> )				C <sub>T</sub> (μmol kg <sup>-1</sup> )				SSS			SST(°C)				
	Min	Max	Mean	STD	Min	Max	Mean	STD	Max	Min	Mean	STD	Max	Min	Mean	STD
Western	323.0	2372.0	2099.4	286.4	397.7	2075.3	1779.6	236.4	34.9	1.1	31.	4.9	30.5	25.5	28.6	0.8
Eastern	1492.9	2320.7	2198.0	141.9	1389.6	2033.0	1892.2	94.2	34.9	22.9	33.6	2.1	29.1	22.8	27.8	1.2

**Table 4.** Root mean square error (rmse) of estimated TA and C<sub>T</sub> from existing relationships.

PARAMETER	REGION	N	REFERENCE	RMSE (μmol kg <sup>-1</sup> )
TA	Western (SSS<35)	392	Lefèvre et al. (2010)	28.6
			Koffi et al. (2010)	64.8
	Eastern (SSS<35)	103	Lefèvre et al. (2010)	28.5
			Koffi et al. (2010)	12.5
	Central (SSS≥35)	1848	Lefèvre et al. (2010)	20.5
			Koffi et al. (2010)	19.2
C <sub>T</sub>	Western (SSS<35)	392	Bonou et al. (2016a)	41.1
			Koffi et al. (2010)	47.9
	Eastern (SSS<35)	103	Bonou et al. (2016a)	29.6
			Koffi et al. (2010)	28.1
	Central (SSS≥35)	1848	Bonou et al. (2016a)	35.1
			Koffi et al. (2010)	34.7

Figure 1

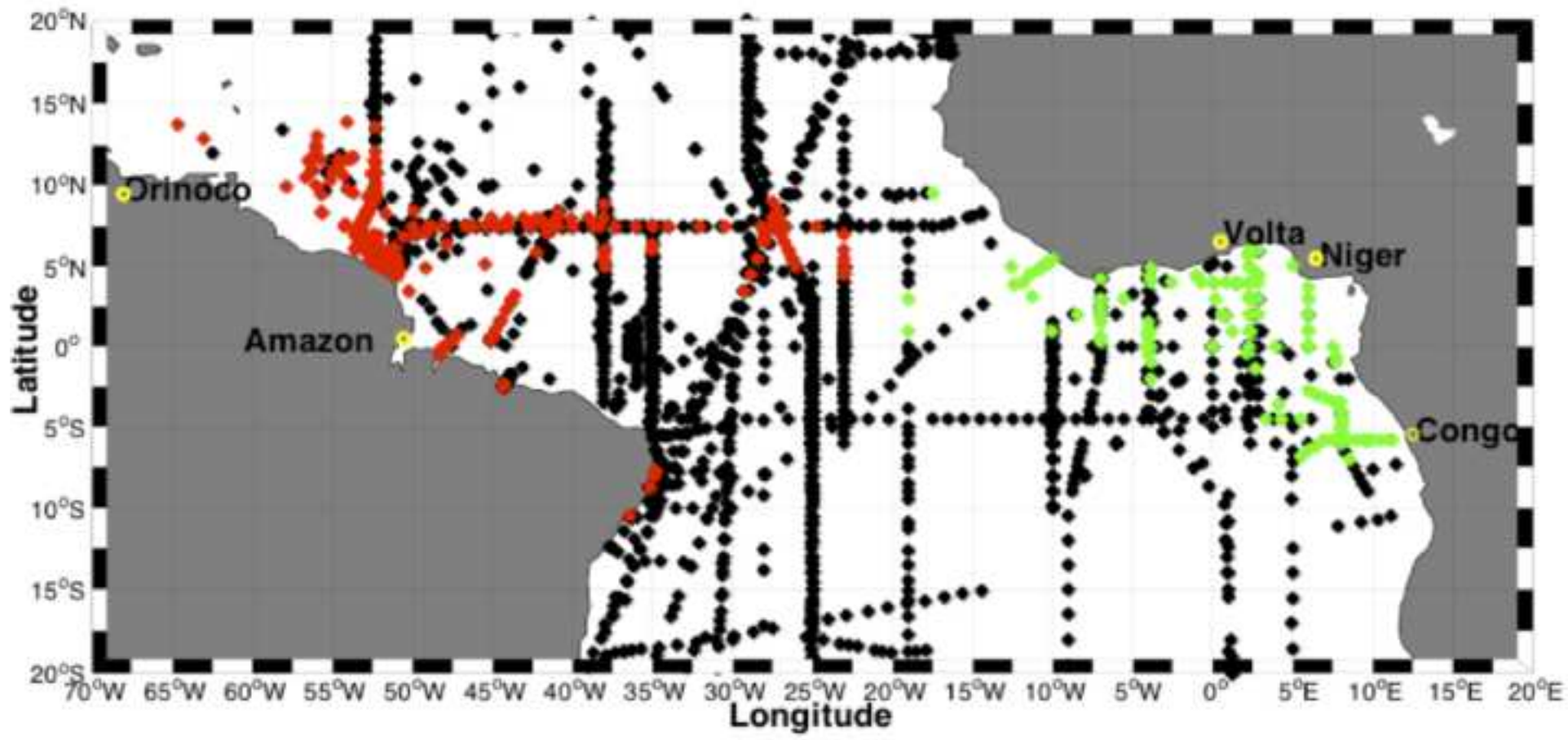


Figure 2

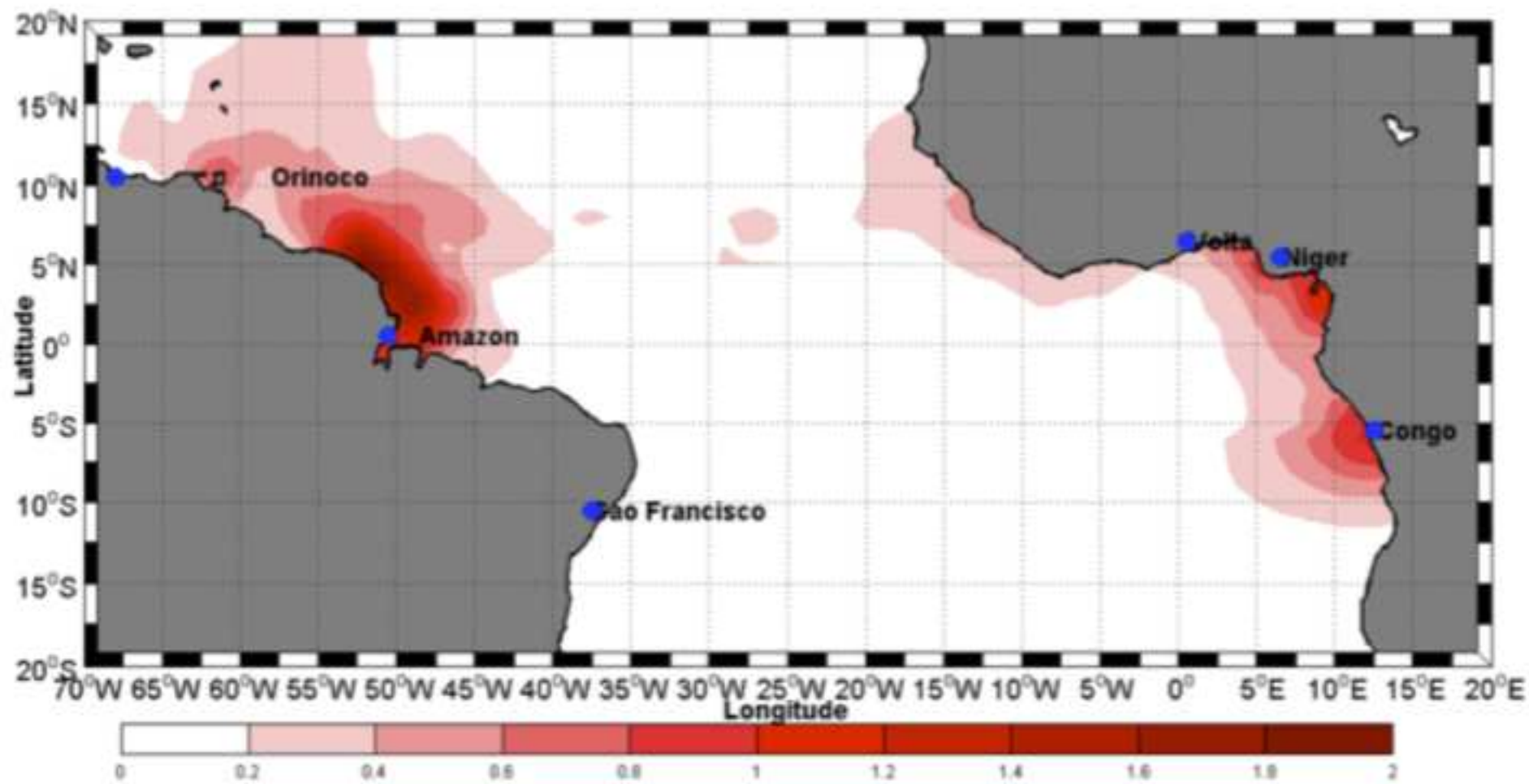




Figure 3

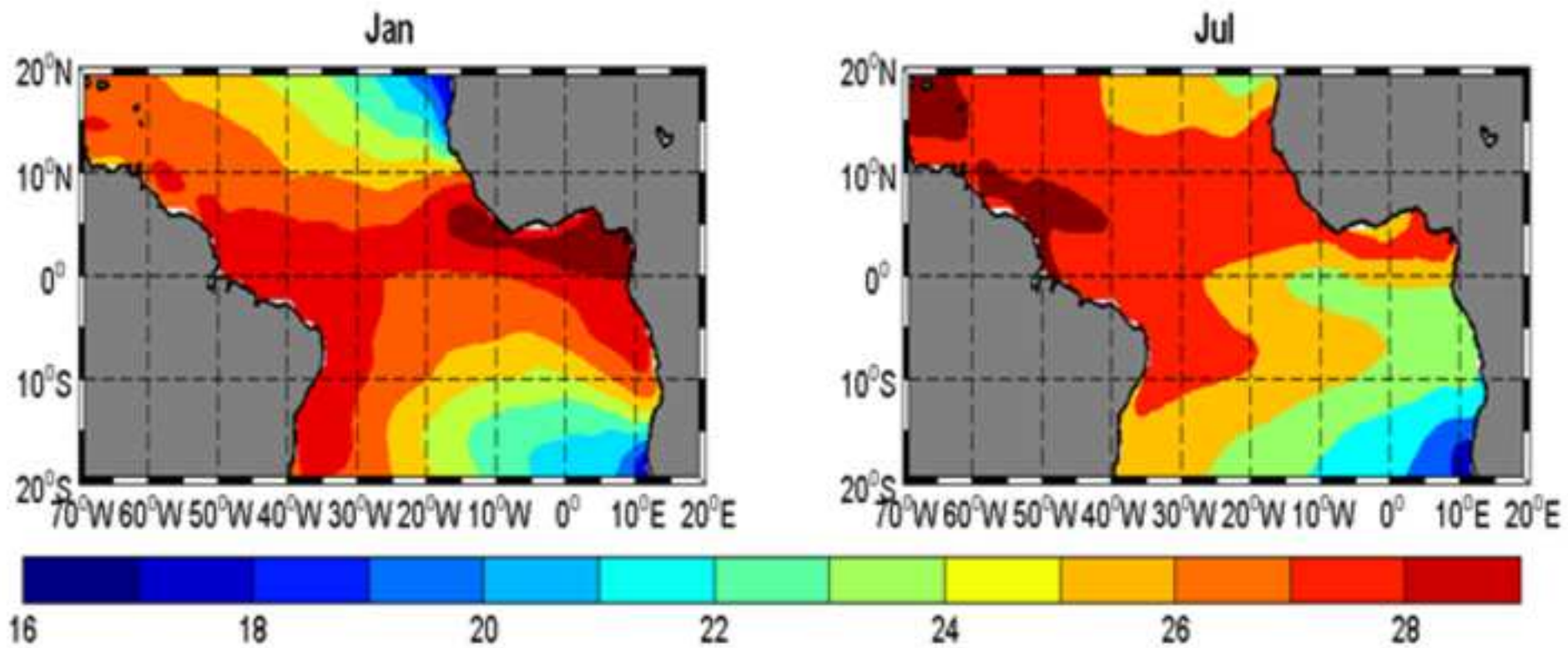


Figure 4

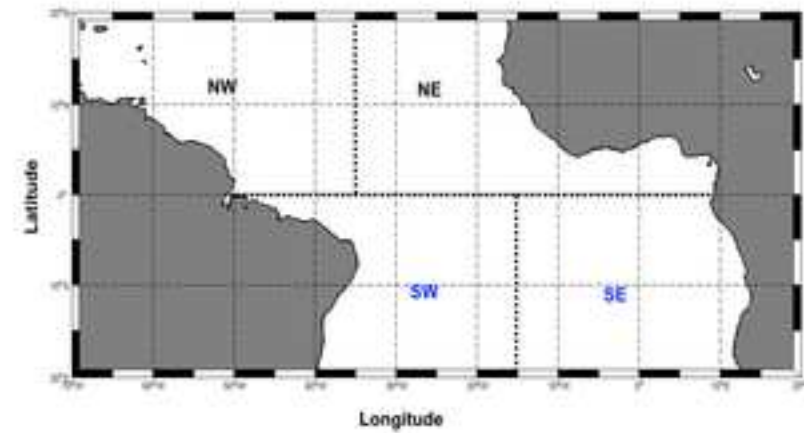
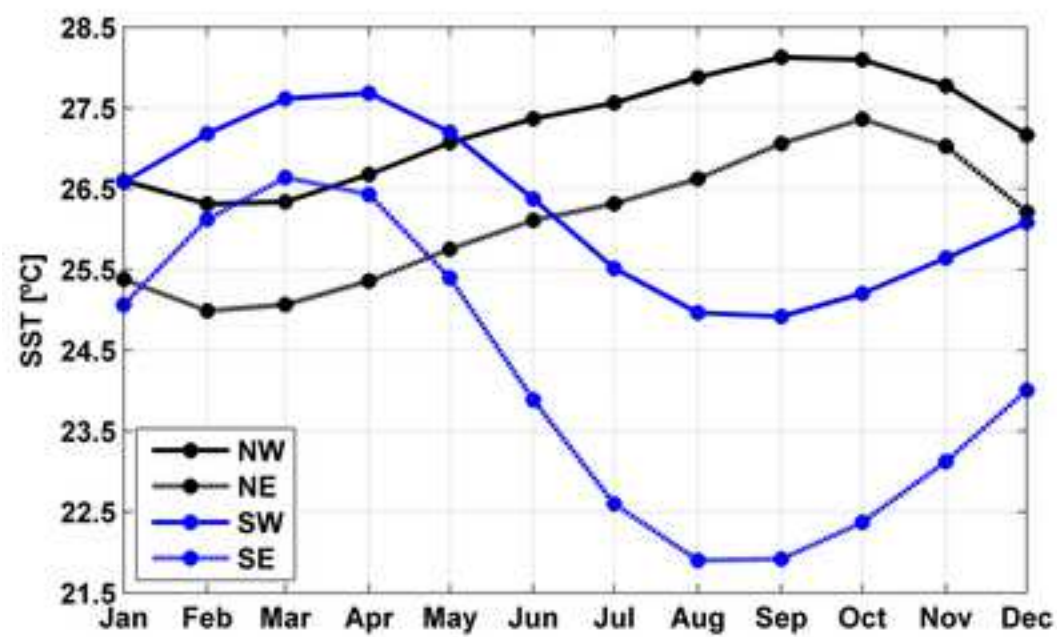


Figure 5

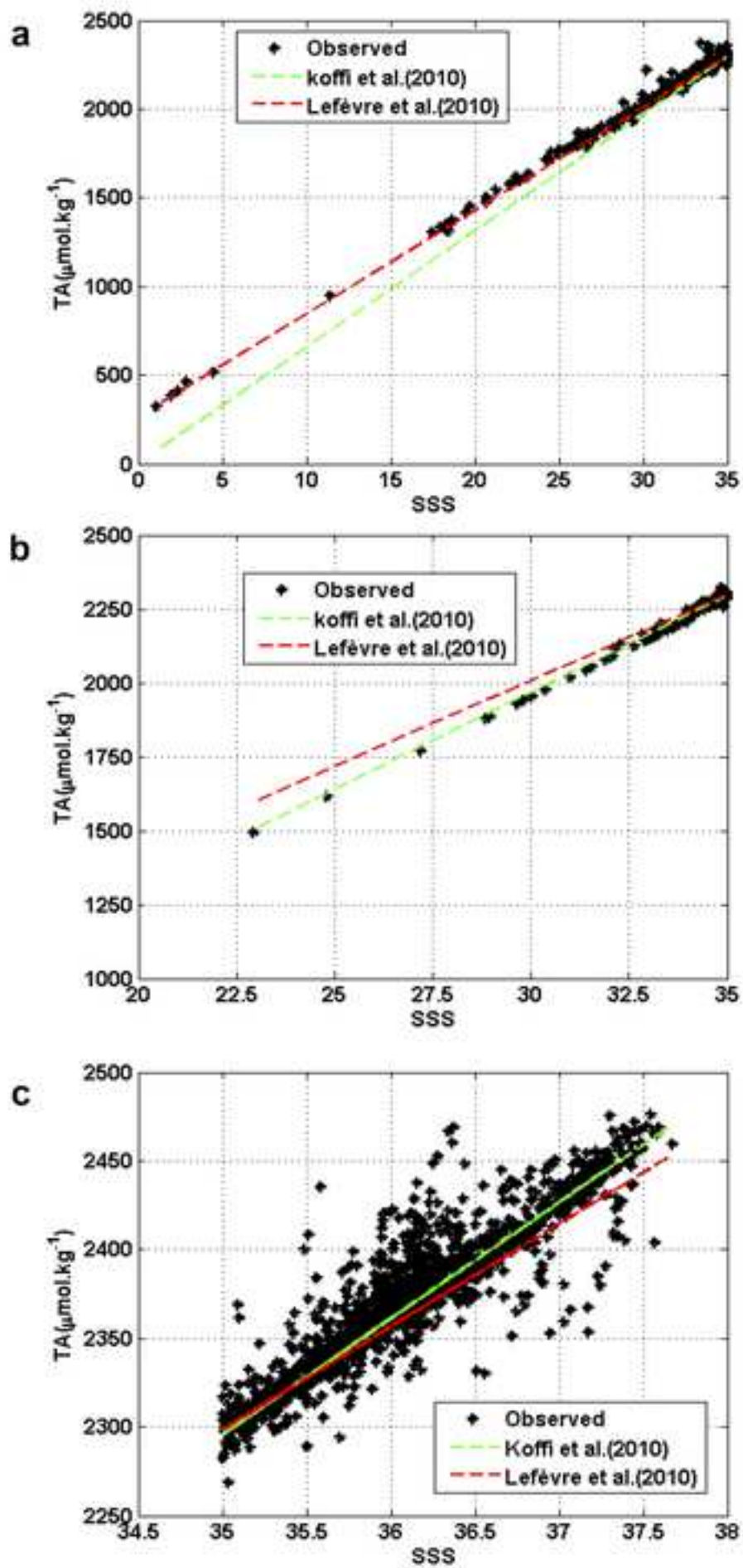


Figure 6

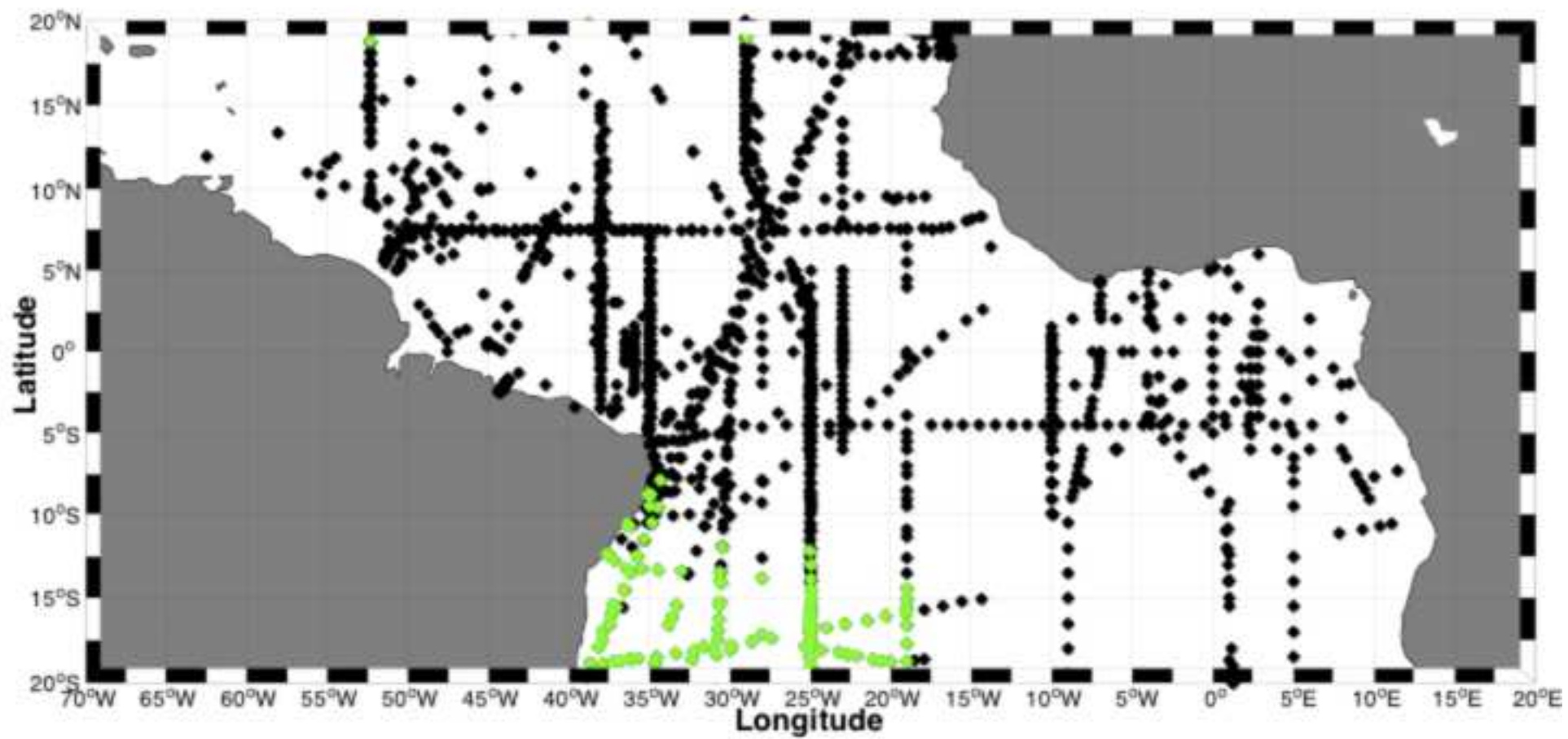


Figure 7

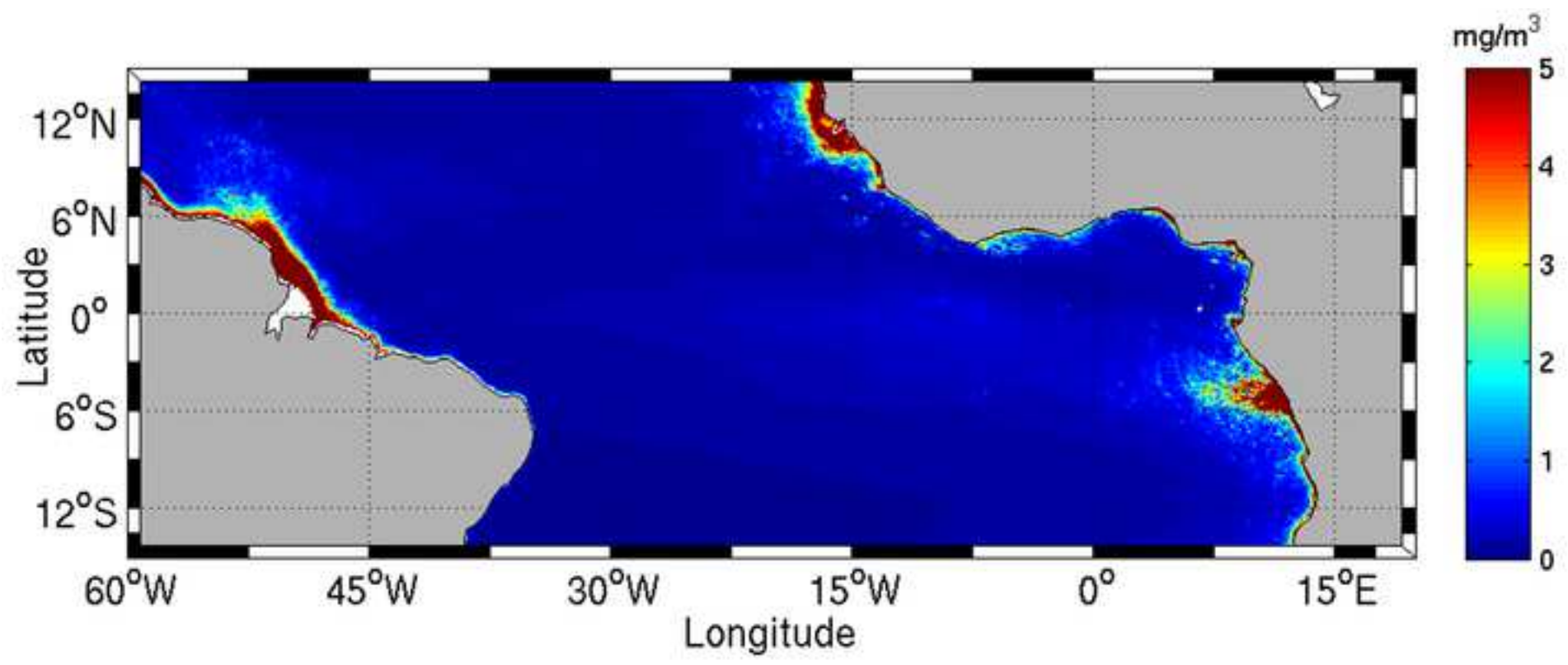


Figure 8

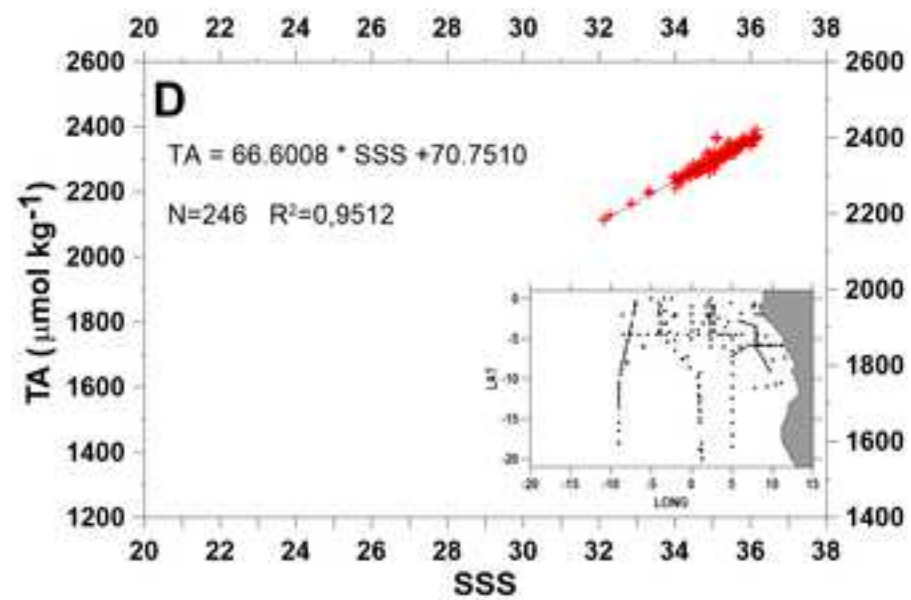
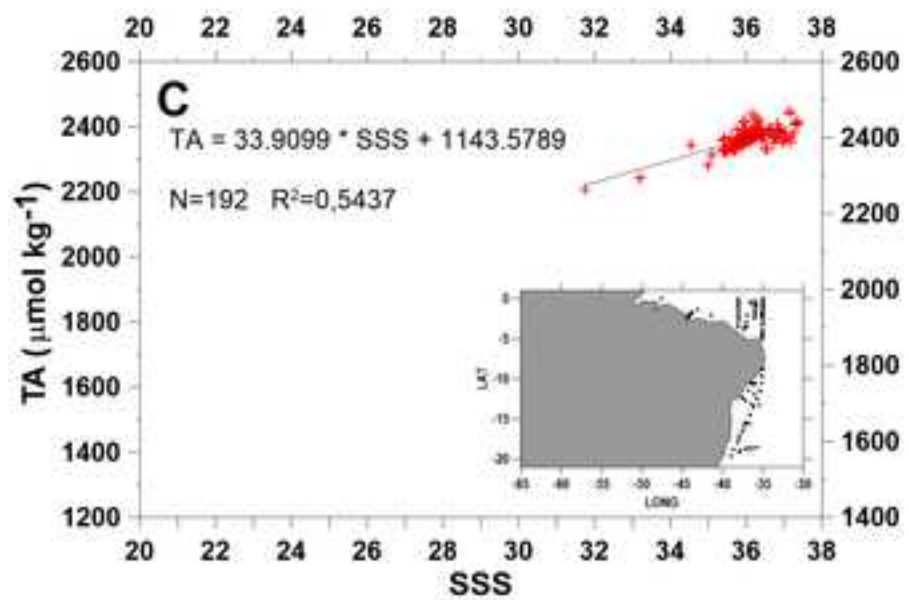
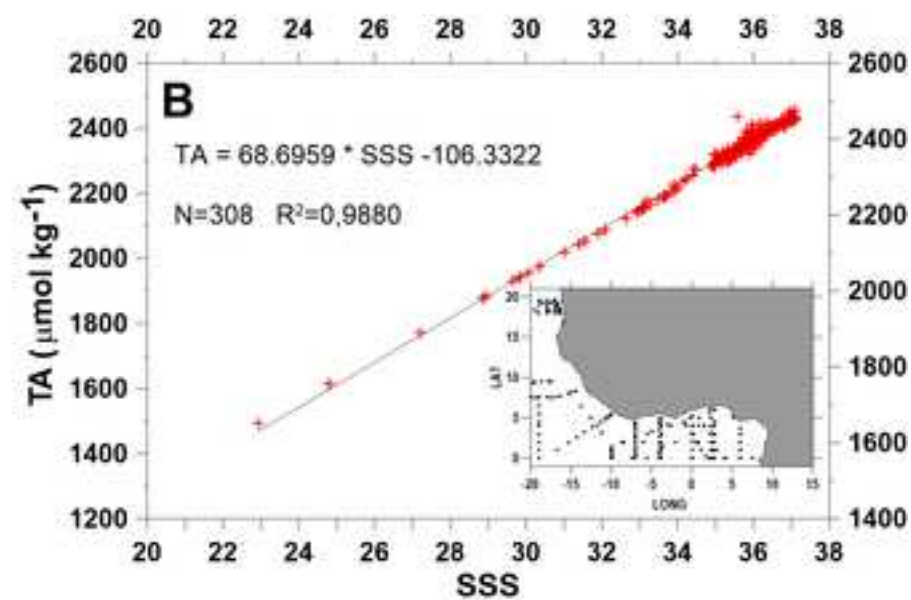
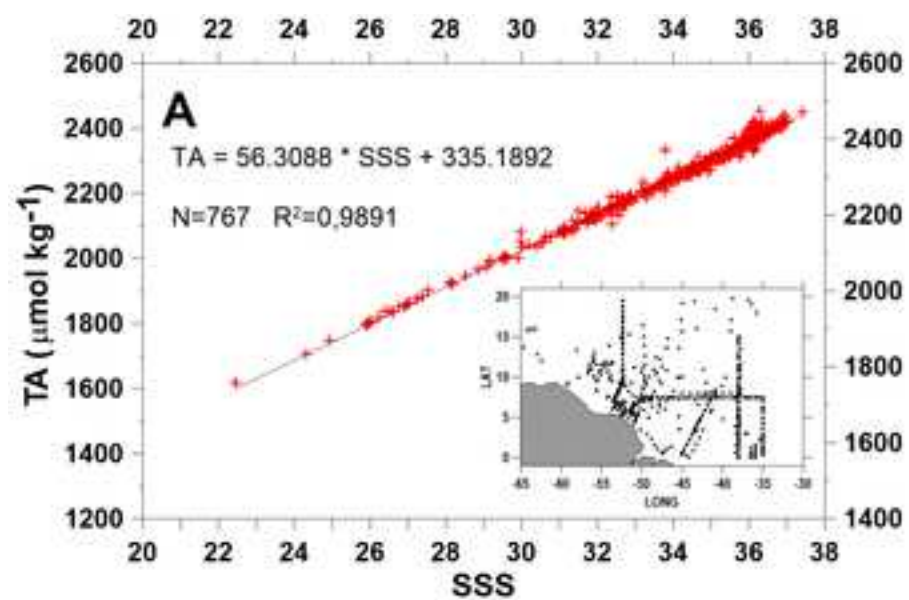


Figure 9

